Towards helicity-dependent parton distribution functions at next-to-next-to-leading order accuracy

based on arXiv:2404.04712

in collaboration with V. Bertone, E. R. Nocera

DIS workshop, Maison MINATEC, Grenoble

Amedeo Chiefa

9th April 2024

THE UNIVERSITY of EDINBURGH

1. Why do we need NNLO?

NNLO – Preparing for the EIC era

NNLO – Preparing for the EIC era

Future improvements

Thus far, only fixed target in polarised DIS experiments

NNLO — Preparing for the EIC era

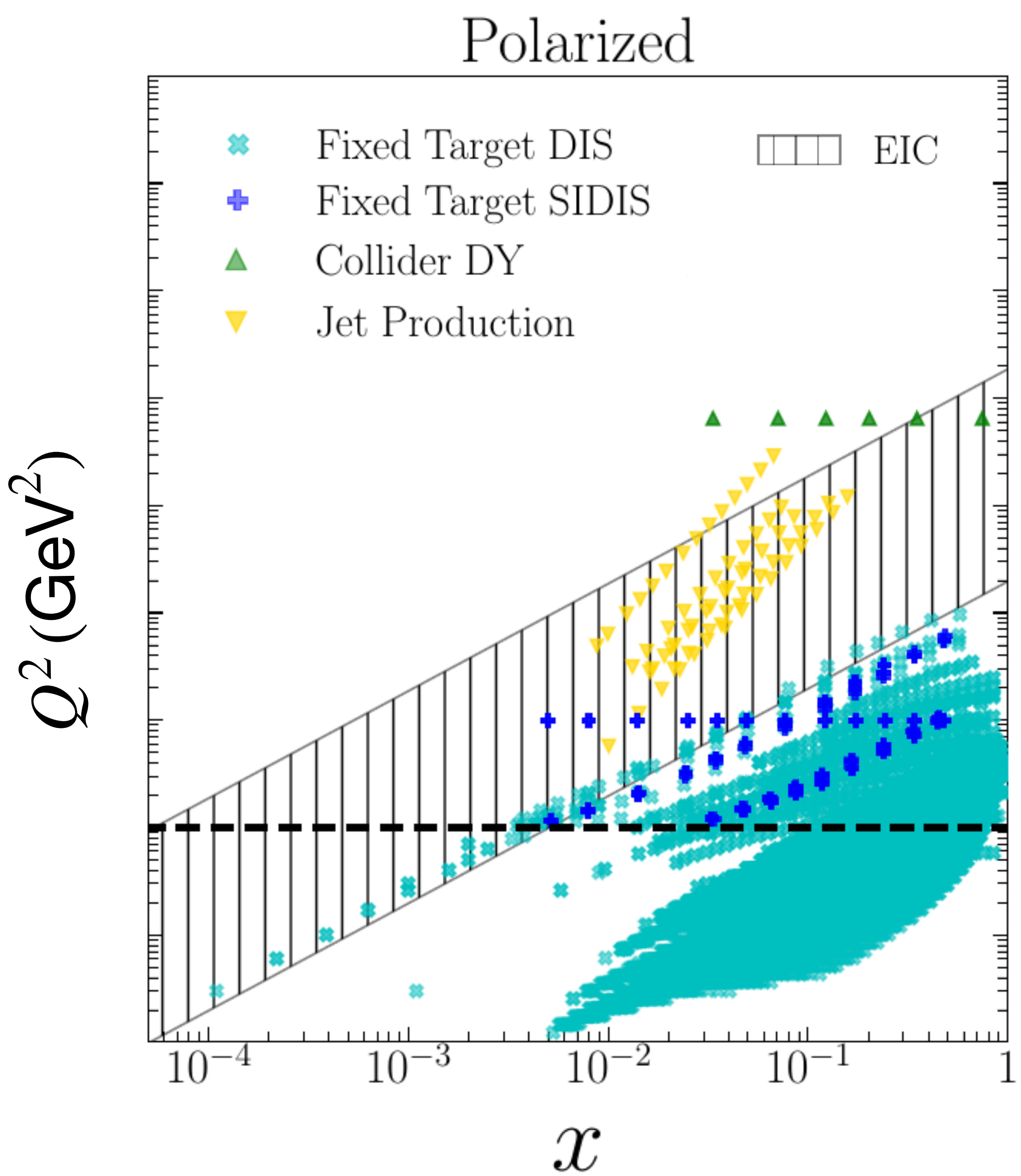

[AR NPS 70 2020 43]

[PRD 102 (2020) 9 094018]

Future improvements

Thus far, only fixed target in polarised DIS experiments

The forthcoming Electron-Ion collider (EIC) will collide polarised proton and lepton beams

NNLO — Preparing for the EIC era

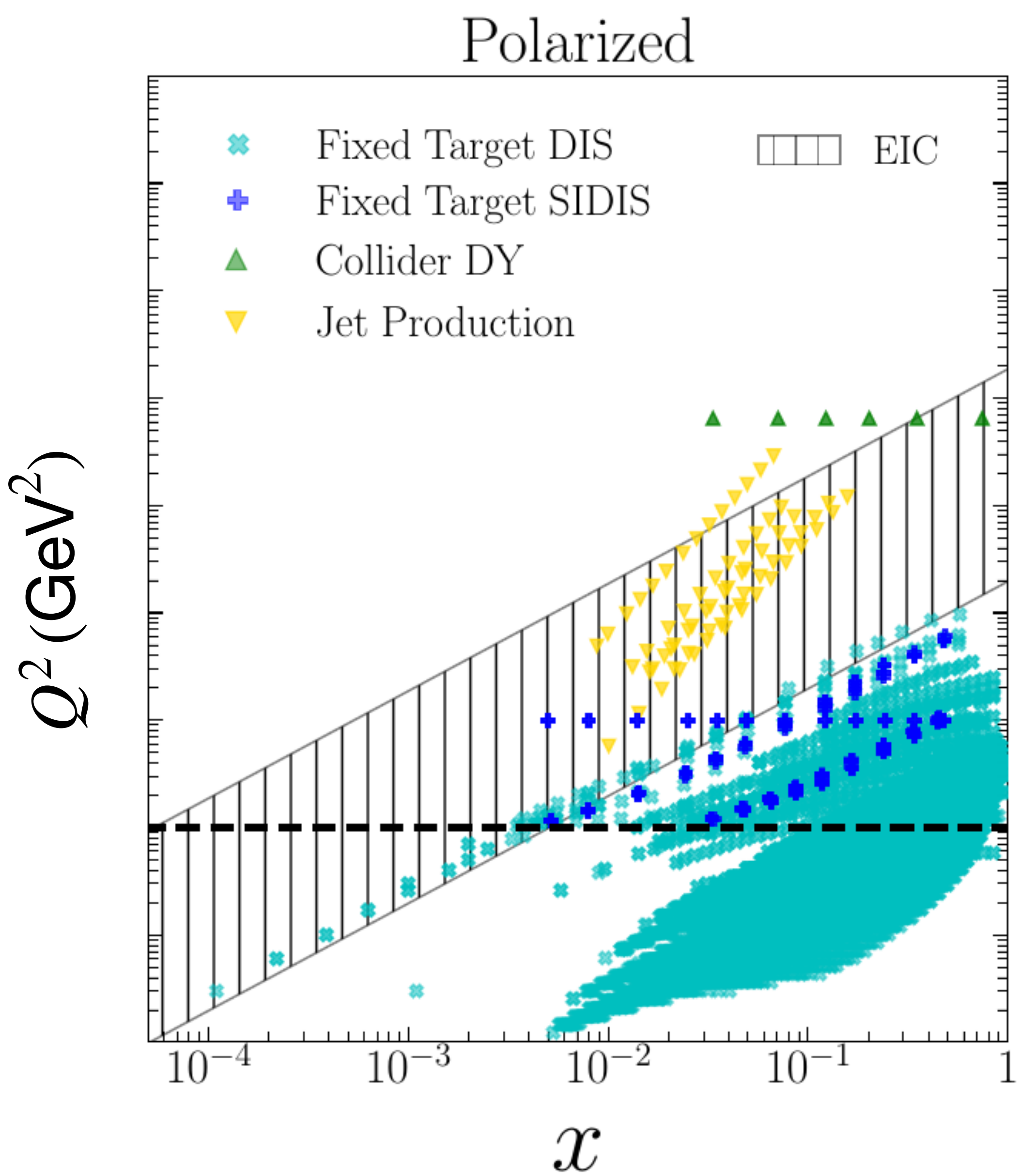

[AR NPS 70 2020 43]

[PRD 102 (2020) 9 094018]

Future improvements

Thus far, only fixed target in polarised DIS experiments

The forthcoming Electron-Ion collider (EIC) will collide polarised proton and lepton beams

Extended kinematic region probed in experiments and increased data availability

NNLO — Preparing for the EIC era

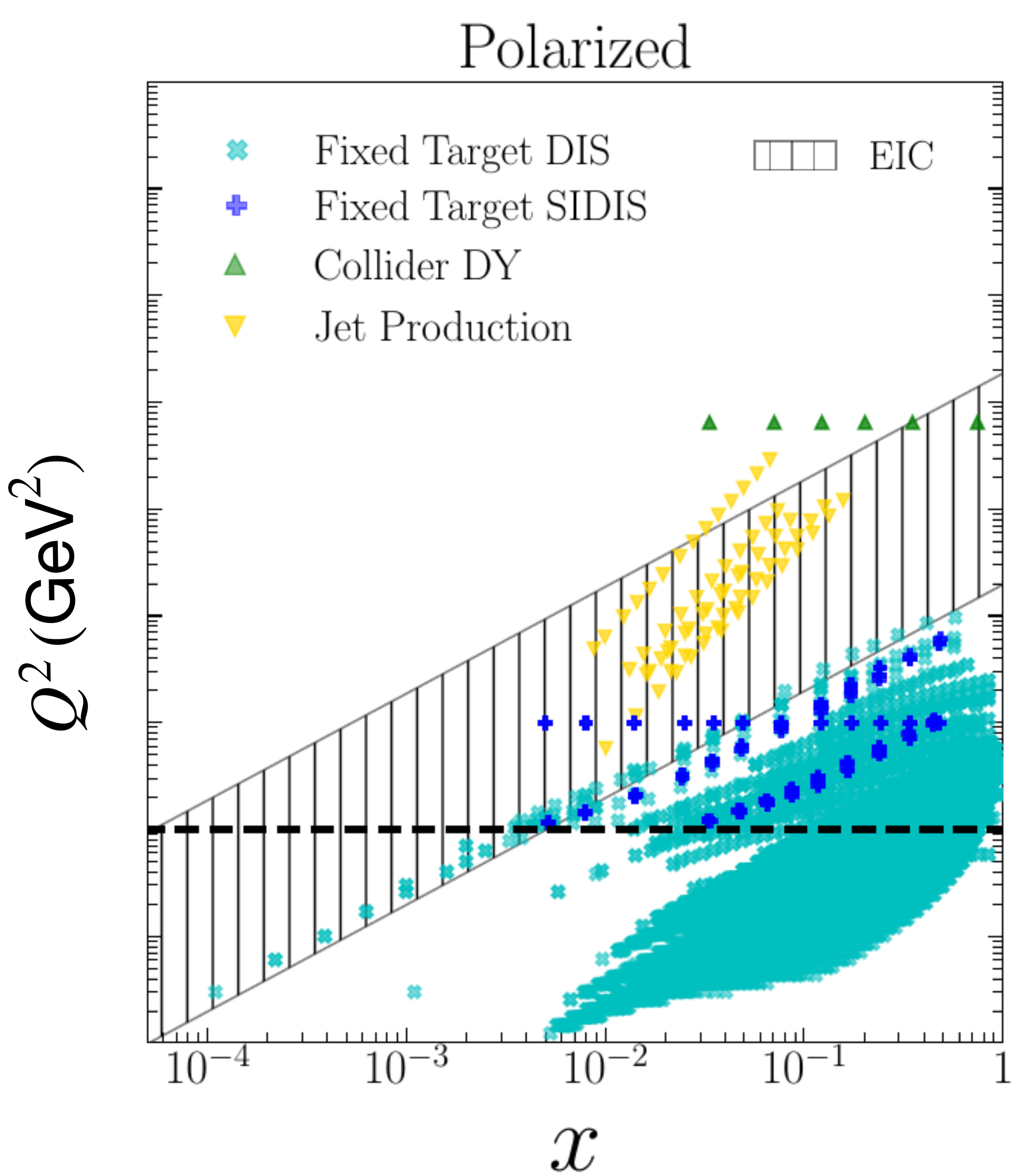

[AR NPS 70 2020 43]

[PRD 102 (2020) 9 094018]

Future improvements

Thus far, only fixed target in polarised DIS experiments

The forthcoming Electron-Ion collider (EIC) will collide polarised proton and lepton beams

Extended kinematic region probed in experiments and increased data availability

EIC aims to improve precision of measurements down to few percent

NNLO — Preparing for the EIC era

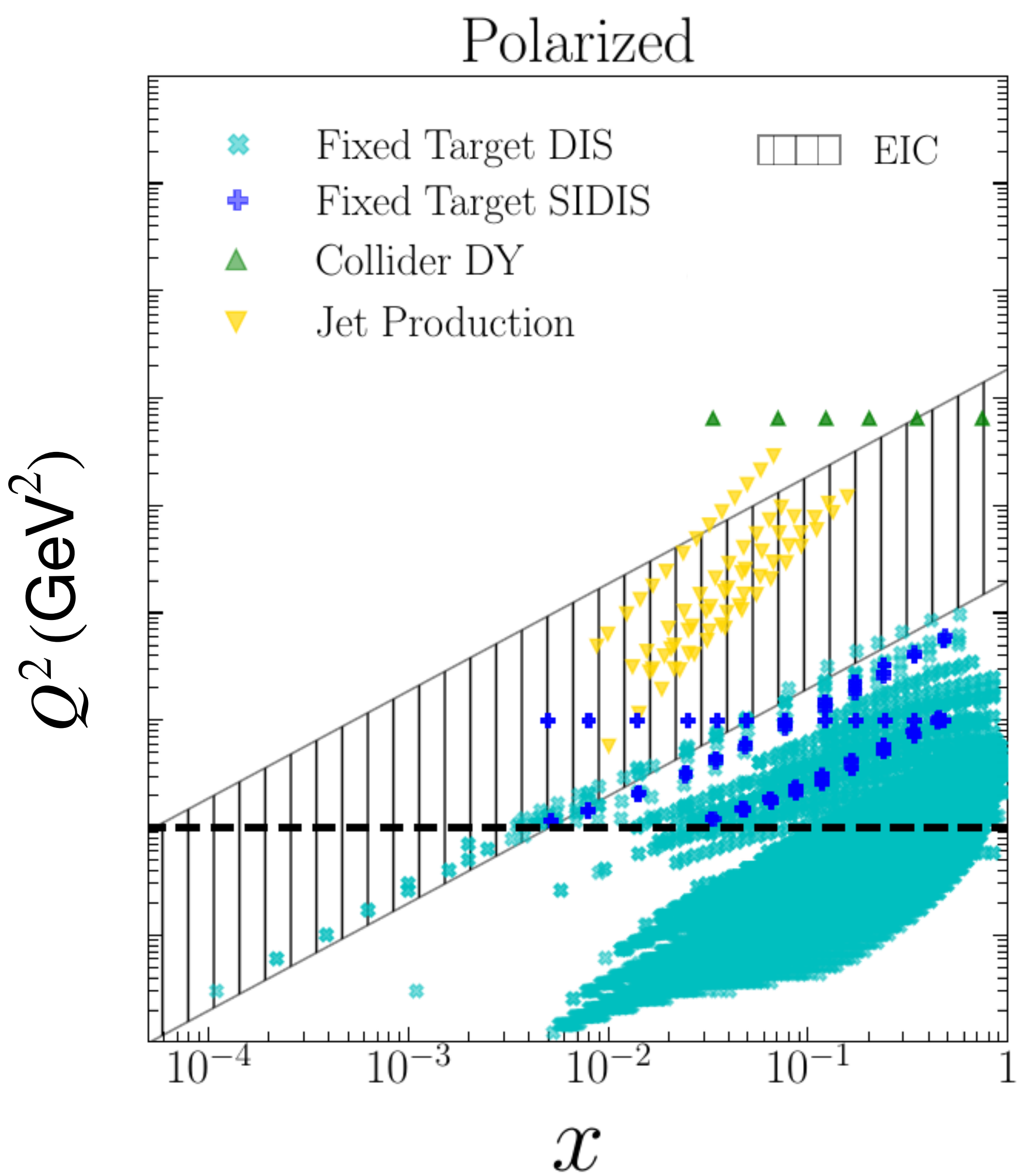

[AR NPS 70 2020 43]

[PRD 102 (2020) 9 094018]

Future improvements

Thus far, only fixed target in polarised DIS experiments

The forthcoming Electron-Ion collider (EIC) will collide polarised proton and lepton beams

Extended kinematic region probed in experiments and increased data availability

EIC aims to improve precision of measurements down to few percent

The theory requirements

NNLO — Preparing for the EIC era

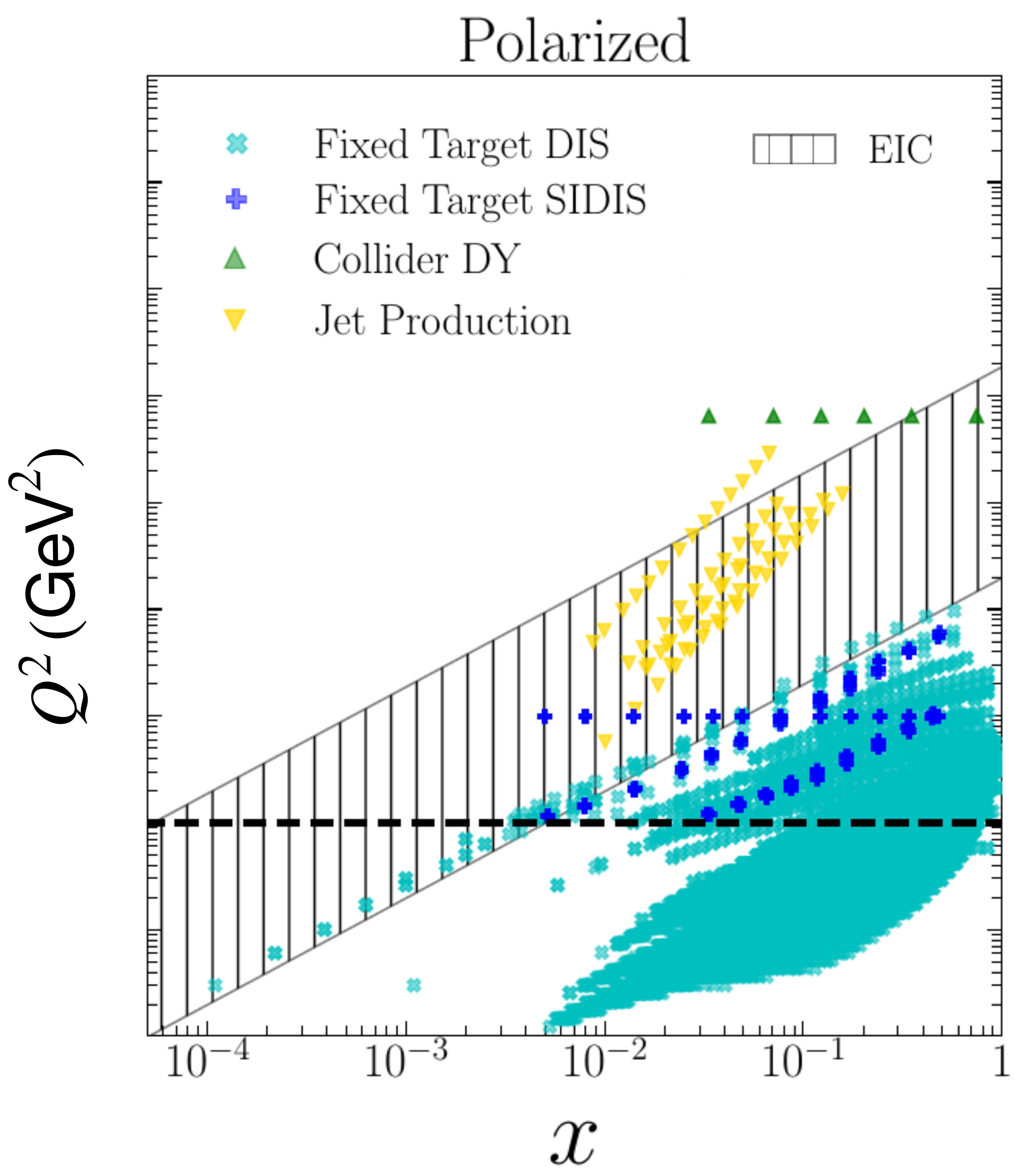

[AR NPS 70 2020 43]

[PRD 102 (2020) 9 094018]

Future improvements

Thus far, only fixed target in polarised DIS experiments

The forthcoming Electron-Ion collider (EIC) will collide polarised proton and lepton beams

Extended kinematic region probed in experiments and increased data availability

EIC aims to improve precision of measurements down to few percent

The theory requirements

Matching accuracy for theoretical predictions by including (more) perturbative corrections

NNLO — Preparing for the EIC era

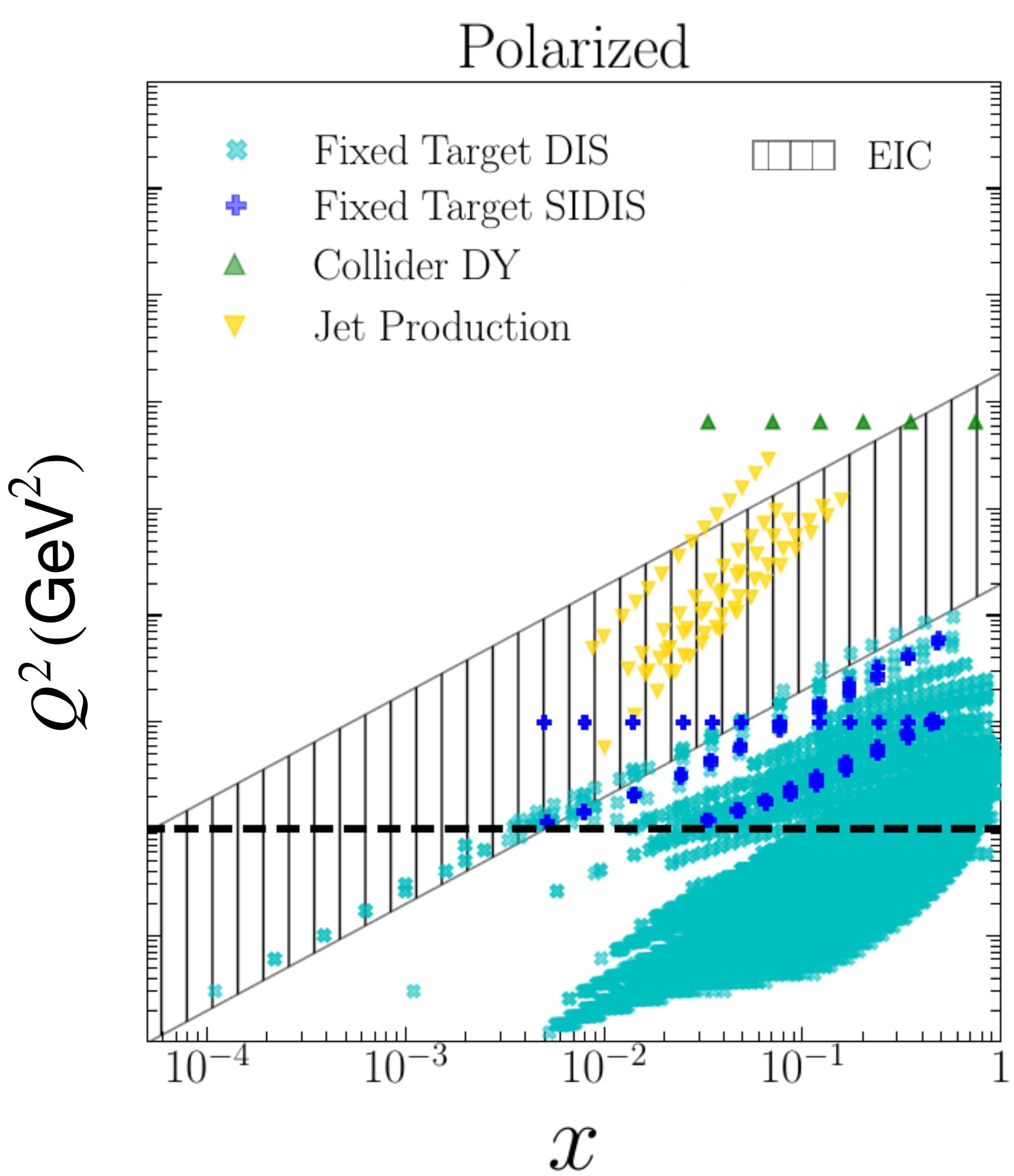

[AR NPS 70 2020 43]

[PRD 102 (2020) 9 094018]

Future improvements

Thus far, only fixed target in polarised DIS experiments

The forthcoming Electron-Ion collider (EIC) will collide polarised proton and lepton beams

Extended kinematic region probed in experiments and increased data availability

EIC aims to improve precision of measurements down to few percent

The theory requirements

Matching accuracy for theoretical predictions by including (more) perturbative corrections

Polarised predictions depend also on the accuracy of polarised PDFs

2. MAPPDFpol1.0

Factorisation of physical observables

Factorisation of physical observables

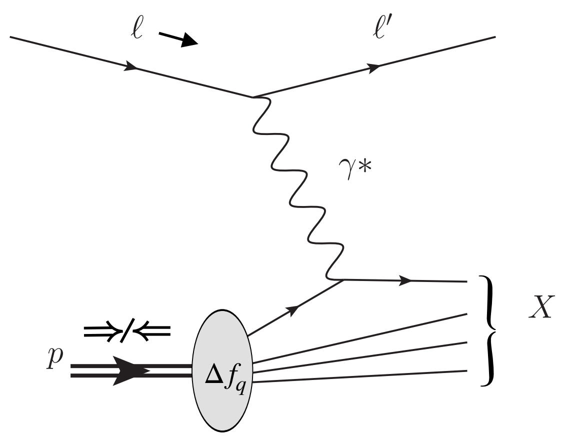

$\ell + N \to \ell' + X$

Deep-inelastic scattering (DIS)

$$\frac{d\Delta\sigma}{dxdy} = \frac{1}{2}\left(\frac{d^2\sigma^{\rightarrow\Rightarrow}}{dxdy} - \frac{d^2\sigma^{\leftarrow\Rightarrow}}{dxdy}\right) = \frac{4\pi\alpha^2}{xQ^2}\left(2-y\right) g_1(x, Q^2)$$

Factorisation of physical observables

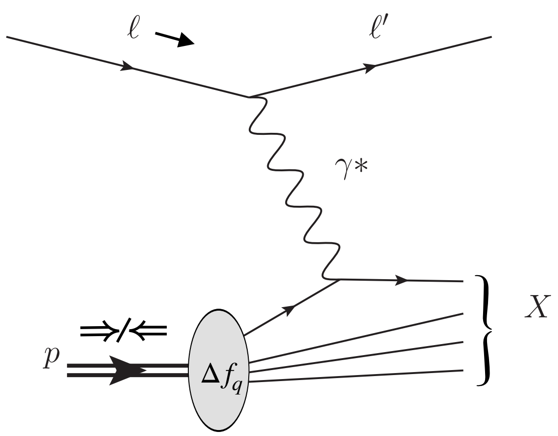

$\ell + N \rightarrow \ell' + X$

Deep-inelastic scattering (DIS)

$$\frac{d\Delta\sigma}{dxdy} = \frac{1}{2}\left(\frac{d^2\sigma^{\rightarrow\Rightarrow}}{dxdy} - \frac{d^2\sigma^{\leftarrow\Rightarrow}}{dxdy}\right) = \frac{4\pi\alpha^2}{xQ^2}\left(2-y\right) g_1(x,Q^2)$$

$$g_1(x,Q^2) = \frac{1}{2}x\sum_q e_q^2 \left\{ \Delta f_q(x,Q^2) \otimes \Delta\mathscr{C}_q(x,Q^2) + \Delta f_g(x,Q^2) \otimes \Delta\mathscr{C}_g(x,Q^2) \right\}$$

Factorisation of physical observables

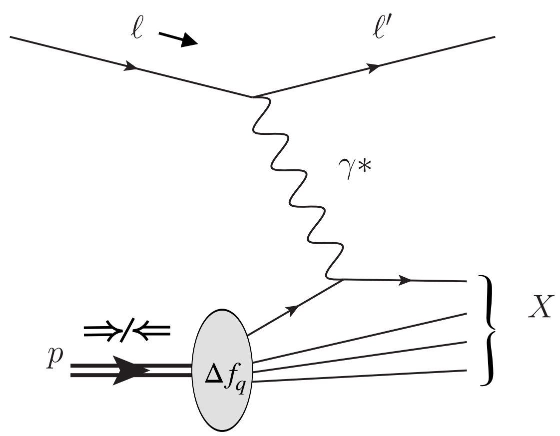

$\ell + N \to \ell' + X$

Deep-inelastic scattering (DIS)

$$\frac{d\Delta\sigma}{dxdy} = \frac{1}{2}\left(\frac{d^2\sigma^{\to\Rightarrow}}{dxdy} - \frac{d^2\sigma^{\leftarrow\Rightarrow}}{dxdy}\right) = \frac{4\pi\alpha^2}{xQ^2}\left(2-y\right) g_1(x,Q^2)$$

$$g_1(x,Q^2) = \frac{1}{2}x\sum_q e_q^2 \left\{ \Delta f_q(x,Q^2) \otimes \Delta\mathscr{C}_q(x,Q^2) + \Delta f_g(x,Q^2) \otimes \Delta\mathscr{C}_g(x,Q^2) \right\}$$

up to NNLO [NPB 417 (1994) 61] } Implemented in APFEL++ and YADISM

Factorisation of physical observables

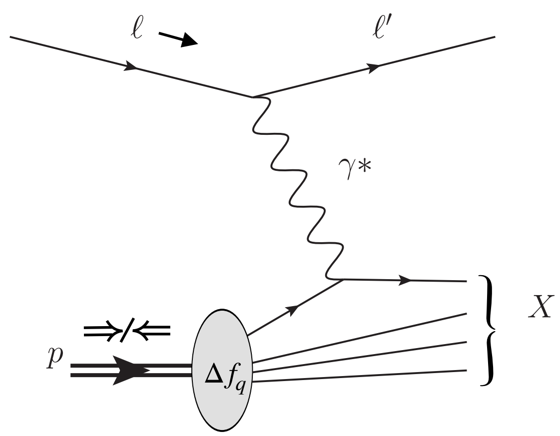

$\ell + N \to \ell' + X$

Deep-inelastic scattering (DIS)

$$\frac{d\Delta\sigma}{dxdy} = \frac{1}{2}\left(\frac{d^2\sigma^{\to\Rightarrow}}{dxdy} - \frac{d^2\sigma^{\leftarrow\Rightarrow}}{dxdy}\right) = \frac{4\pi\alpha^2}{xQ^2}(2-y)\, g_1(x,Q^2)$$

$$g_1(x,Q^2) = \frac{1}{2}x\sum_q e_q^2 \left\{ \Delta f_q(x,Q^2) \otimes \Delta\mathscr{C}_q(x,Q^2) + \Delta f_g(x,Q^2) \otimes \Delta\mathscr{C}_g(x,Q^2) \right\}$$

up to NNLO [NPB 417 (1994) 61] } Implemented in APFEL++ and YADISM

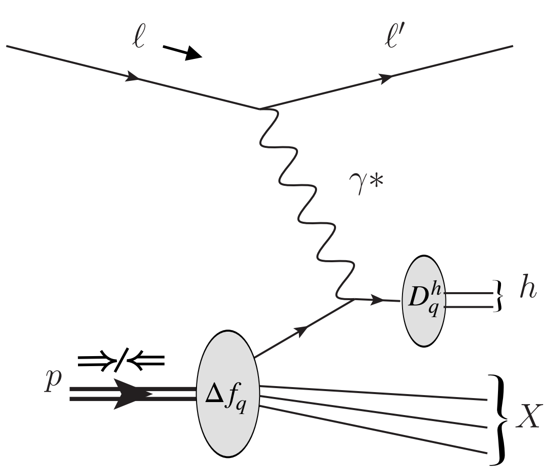

$\ell + N \to \ell' + h + X$

Semi-inclusive deep-inelastic scattering (SIDIS)

$$\frac{d\Delta\sigma^h}{dxdy} = \frac{1}{2}\left(\frac{d^3\sigma_h^{\to\Rightarrow}}{dxdy} - \frac{d^3\sigma_h^{\leftarrow\Rightarrow}}{dxdy}\right) = \frac{4\pi\alpha^2}{xQ^2}(2-y)\, g_1^h(x,z,Q^2)$$

Factorisation of physical observables

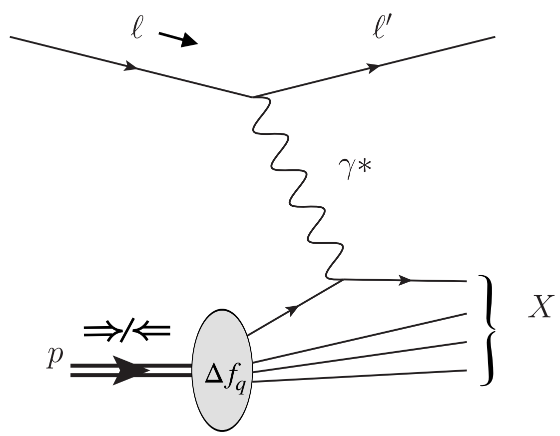

$\ell + N \rightarrow \ell' + X$

Deep-inelastic scattering (DIS)

$$\frac{d\Delta\sigma}{dxdy} = \frac{1}{2}\left(\frac{d^2\sigma^{\rightarrow\Rightarrow}}{dxdy} - \frac{d^2\sigma^{\leftarrow\Rightarrow}}{dxdy}\right) = \frac{4\pi\alpha^2}{xQ^2}\,(2-y)\,g_1(x,Q^2)$$

$$g_1(x,Q^2) = \frac{1}{2}x\sum_q e_q^2\left\{\Delta f_q(x,Q^2)\otimes\Delta\mathscr{C}_q(x,Q^2) + \Delta f_g(x,Q^2)\otimes\Delta\mathscr{C}_g(x,Q^2)\right\}$$

up to NNLO [NPB 417 (1994) 61] — Implemented in APFEL++ and YADISM

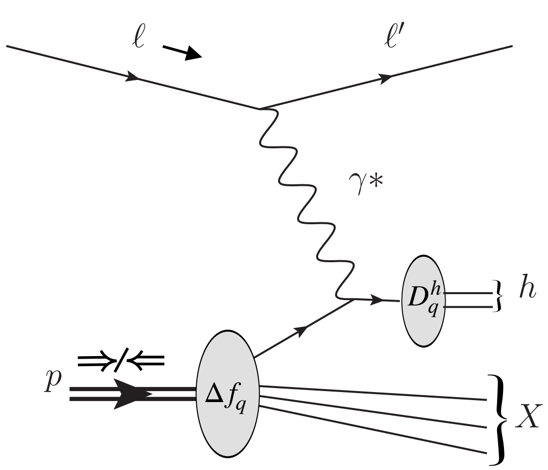

$\ell + N \rightarrow \ell' + h + X$

Semi-inclusive deep-inelastic scattering (SIDIS)

$$\frac{d\Delta\sigma^h}{dxdy} = \frac{1}{2}\left(\frac{d^3\sigma_h^{\rightarrow\Rightarrow}}{dxdy} - \frac{d^3\sigma_h^{\leftarrow\Rightarrow}}{dxdy}\right) = \frac{4\pi\alpha^2}{xQ^2}\,(2-y)\,g_1^h(x,z,Q^2)$$

$$g_1^h(x,z,Q^2) = \frac{1}{2}x\sum_q e_q^2\left\{\left[\Delta f_q(x,Q^2)\underset{x}{\otimes}\Delta\mathscr{C}_{qq}(x,z,Q^2) + \Delta f_g(x,Q^2)\underset{x}{\otimes}\Delta\mathscr{C}_{qg}(x,z,Q^2)\right]\underset{z}{\otimes} D_q^h(z,Q^2)\right.$$

$$\left.\Delta f_q(x,Q^2)\underset{x}{\otimes}\Delta\mathscr{C}_{gq}\underset{z}{\otimes} D_g^h(z,Q^2)\right\},$$

Factorisation of physical observables

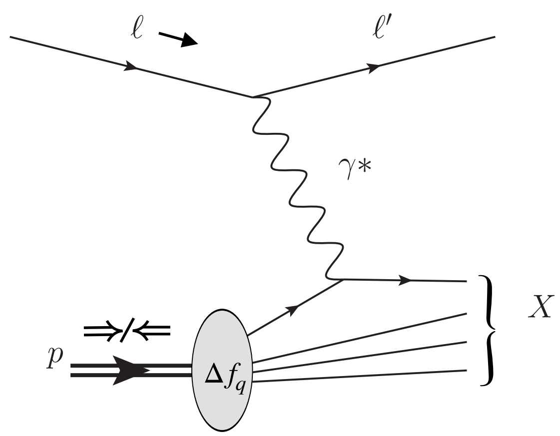

$\ell + N \rightarrow \ell' + X$

Deep-inelastic scattering (DIS)

$$\frac{d\Delta\sigma}{dxdy} = \frac{1}{2}\left(\frac{d^2\sigma^{\rightarrow\Rightarrow}}{dxdy} - \frac{d^2\sigma^{\leftarrow\Rightarrow}}{dxdy}\right) = \frac{4\pi\alpha^2}{xQ^2}\,(2-y)\, g_1(x,Q^2)$$

$$g_1(x,Q^2) = \frac{1}{2}x\sum_q e_q^2\left\{\Delta f_q(x,Q^2)\otimes\Delta\mathscr{C}_q(x,Q^2) + \Delta f_g(x,Q^2)\otimes\Delta\mathscr{C}_g(x,Q^2)\right\}$$

up to NNLO [NPB 417 (1994) 61] } Implemented in APFEL++ and YADISM

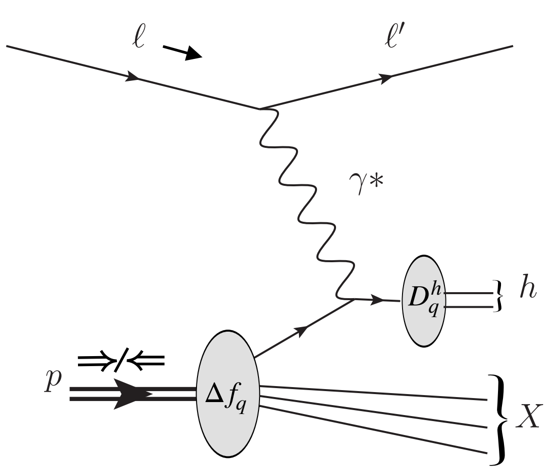

$\ell + N \rightarrow \ell' + h + X$

Semi-inclusive deep-inelastic scattering (SIDIS)

$$\frac{d\Delta\sigma^h}{dxdy} = \frac{1}{2}\left(\frac{d^3\sigma_h^{\rightarrow\Rightarrow}}{dxdy} - \frac{d^3\sigma_h^{\leftarrow\Rightarrow}}{dxdy}\right) = \frac{4\pi\alpha^2}{xQ^2}\,(2-y)\, g_1^h(x,z,Q^2)$$

$$g_1^h(x,z,Q^2) = \frac{1}{2}x\sum_q e_q^2\left\{\left[\Delta f_q(x,Q^2)\underset{x}{\otimes}\Delta\mathscr{C}_{qq}(x,z,Q^2) + \Delta f_g(x,Q^2)\underset{x}{\otimes}\Delta\mathscr{C}_{qg}(x,z,Q^2)\right]\underset{z}{\otimes} D_q^h(z,Q^2)\right.$$
$$\left.\Delta f_q(x,Q^2)\underset{x}{\otimes}\Delta\mathscr{C}_{gq}\underset{z}{\otimes}D_g^h(z,Q^2)\right\},$$

up to NLO [NPB 160 (1979) 301; PRD 57 (1998) 5811]
approximate NNLO [PRD 104 094046] } Implemented in APFEL++

FFs for $\pi^{\pm}, K^{\pm}$: MAPFF1.0 [PRD 104 034007]

No massive-quark corrections and perturbative charm in ZM-VFNS.

The data set

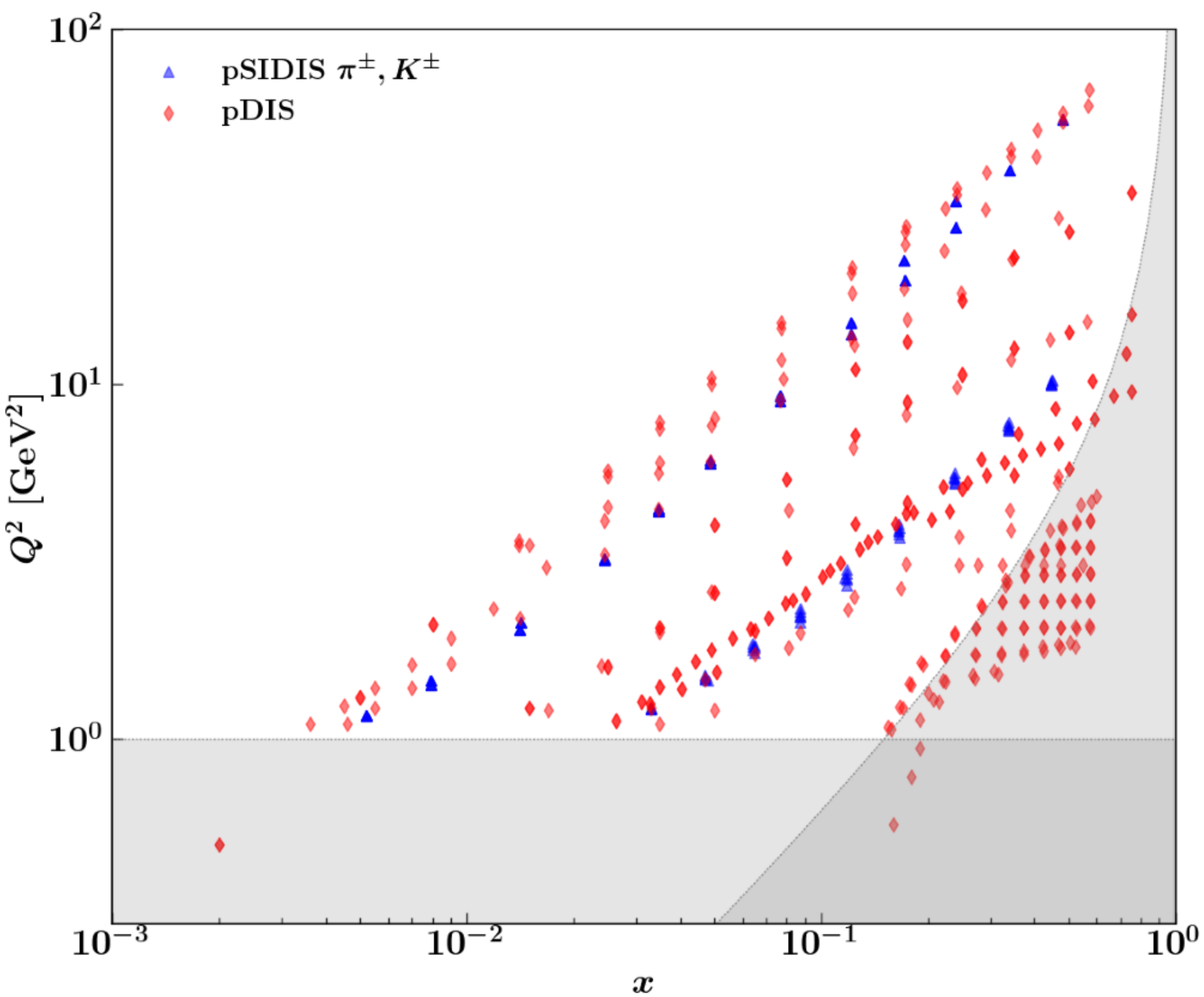

Kinematic cuts

$Q^2 > 1\,\text{GeV}^2$ $\quad$ $W^2 > 6.25\,\text{GeV}^2$

Data set	Obs.	N_{dat}	Reference
E142	g_1^n	8 (7)	[PRD 54 (1996) 6620]
E143	g_1^p	28 (25)	[PRD 58 (1996) 112003]
	g_1^d	28 (25)	
E154	g_1^n	11	[PRL 79 (1997 26)]
E155	g_1^p/F_1^p	24 (22)	[PRL 493 (2000) 19]
	g_1^n/F_1^n	24 (22)	
EMC	g_1^p	10	[NPB 328 (1989) 1]
SMC	g_1^d	13 (12)	[PRD D58 (1998) 112001]
	g_1^p	13 (12)	
JLAB E06 014	g_1^n/F_1^n	6 (1)	[PRD 94.5 (2016) 052003]
JLAB E97 103	g_1^n	5 (0)	[AIP CP 675.1 (2003) 615]
JLAB E99 117	g_1^n/F_1^n	3 (0)	[PRD 94.5 (2016) 052003]
JLAB EG1 DVCS	g_1^p/F_1^p	44 (1)	[PRC 90.2 (2014) 025212]
	g_1^d/F_1^d	47 (2)	
COMPASS	g_1^p	17	[PLB 753 (2016) 18]
	g_1^d	15	[PLB 769 (2017) 34]
HERMES	g_1^p	15 (14)	[PRD 75 (2007) 012007]
	g_1^d	15 (14)	
	g_1^n	9 (8)	[PLB 404 (1997) 383]
COMPASS	$g_{1,p,d}^{K^+}/F_{1,p,d}^{K^+}$	22	[PLB 680 (2009) 217]
	$g_{1,p,d}^{K^-}/F_{1,p,d}^{K^-}$	22	
	$g_{1,p,d}^{\pi^+}/F_{1,p,d}^{\pi^+}$	22	
	$g_{1,p,d}^{\pi^-}/F_{1,p,d}^{\pi^-}$	22	
HERMES	$g_{1,p,d}^{\pi^+}/F_{1,p,d}^{\pi^+}$	18	[PRD 99 (2019) 112001]
	$g_{1,p,d}^{\pi^-}/F_{1,p,d}^{\pi^-}$	18	
	$g_{1,d}^{K^+}/F_{1,d}^{K^+}$	9	
	$g_{1,d}^{K^+}/F_{1,d}^{K^+}$	9	
Total		477 (362)	

The methodology

The methodology

Monte Carlo propagation of data uncertainties into PDF uncertainties ($N_{rep} = 150$)

The methodology

Monte Carlo propagation of data uncertainties into PDF uncertainties ($N_{rep} = 150$)

PDFs parametrised with a feed-forward Neural Network

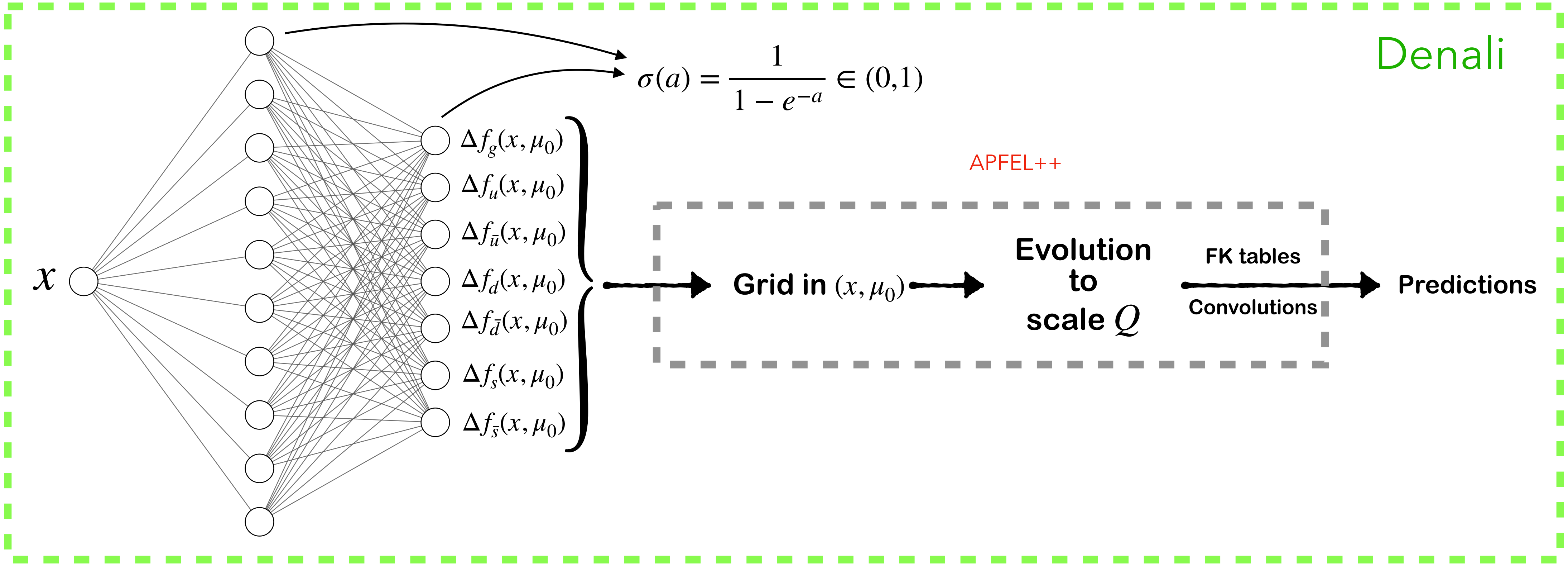

The methodology

Monte Carlo propagation of data uncertainties into PDF uncertainties ($N_{rep} = 150$)

PDFs parametrised with a feed-forward Neural Network

Parametrisation basis at $Q^2 = 1\,\mathrm{GeV}^2$: $\{\Delta f_u, \Delta f_{\bar{u}}, \Delta f_d, \Delta f_{\bar{d}}, \Delta f_s, \Delta f_{\bar{s}}, \Delta f_g\}$

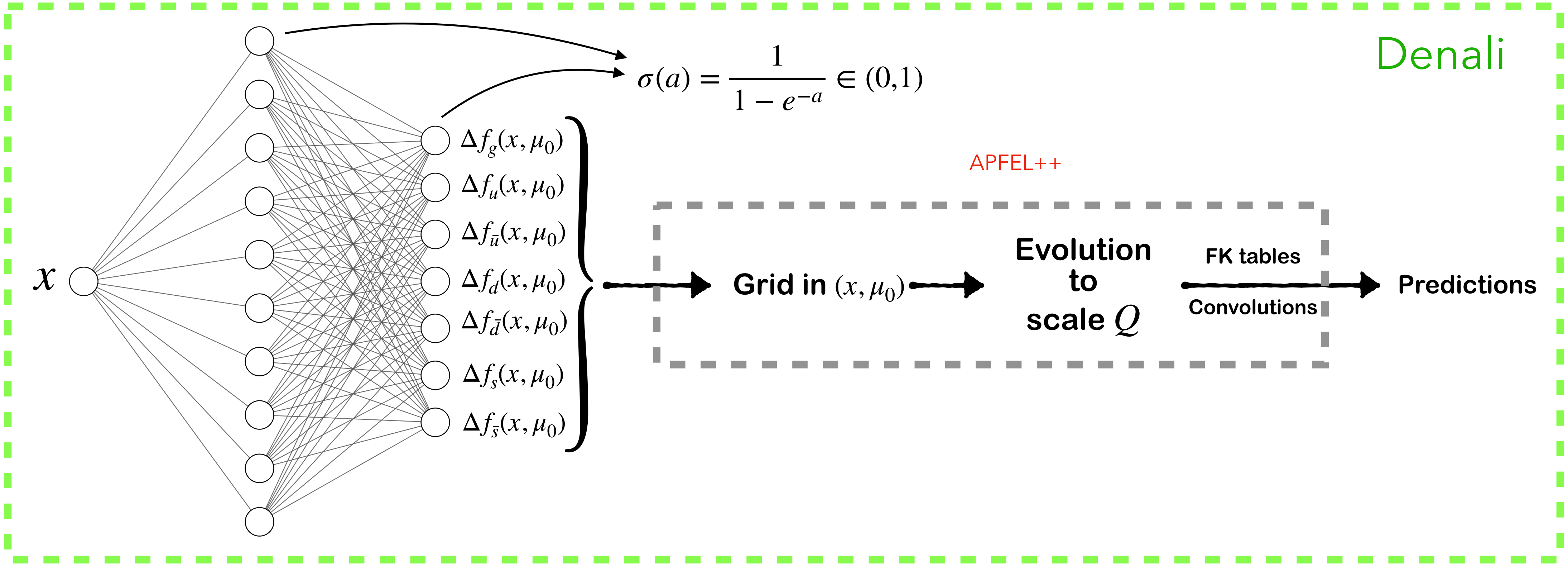

The methodology

Monte Carlo propagation of data uncertainties into PDF uncertainties ($N_{rep} = 150$)

PDFs parametrised with a feed-forward Neural Network

Parametrisation basis at $Q^2 = 1$ GeV^2 : $\{\Delta f_u, \Delta f_{\bar{u}}, \Delta f_d, \Delta f_{\bar{d}}, \Delta f_s, \Delta f_{\bar{s}}, \Delta f_g\}$

Levenberg-Marquardt for minimisation and cross-validation to avoid over-learning

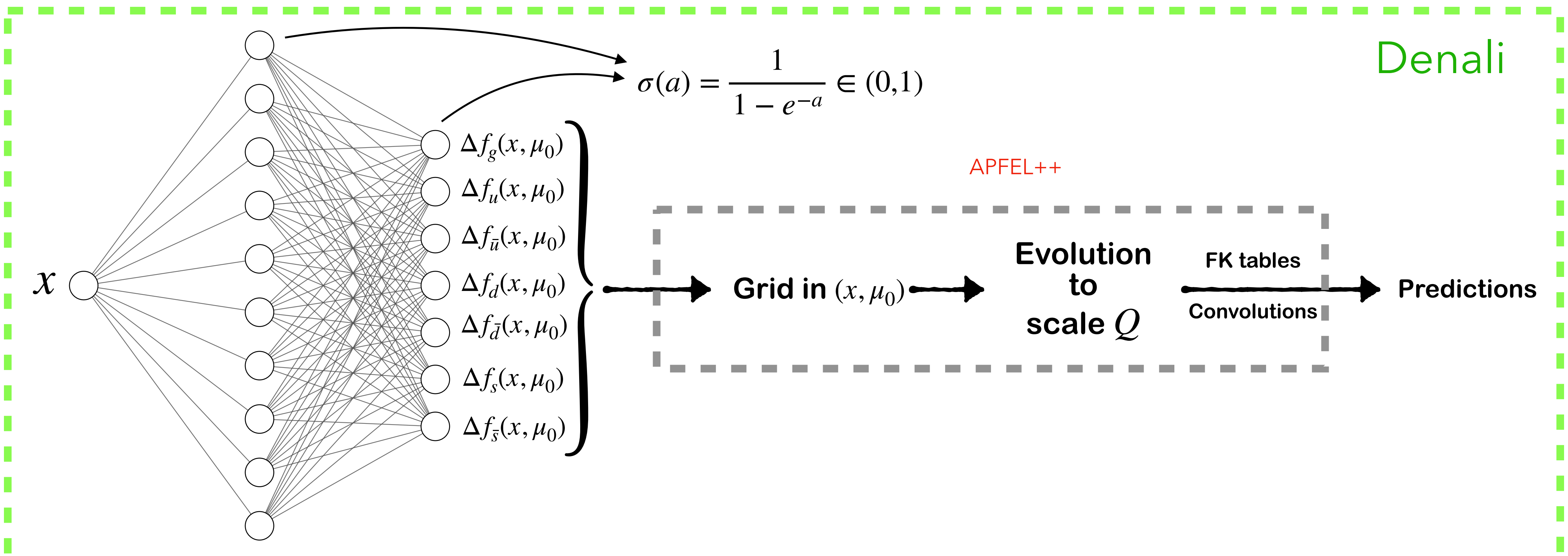

The methodology

Monte Carlo propagation of data uncertainties into PDF uncertainties ($N_{rep} = 150$)

PDFs parametrised with a feed-forward Neural Network

Parametrisation basis at $Q^2 = 1\,\text{GeV}^2$: $\{\Delta f_u, \Delta f_{\bar{u}}, \Delta f_d, \Delta f_{\bar{d}}, \Delta f_s, \Delta f_{\bar{s}}, \Delta f_g\}$

Levenberg-Marquardt for minimisation and cross-validation to avoid over-learning

Predictions computed with APFEL++ library [CPC 212 (2017) 205; PoS DIS2017 (2018) 201]

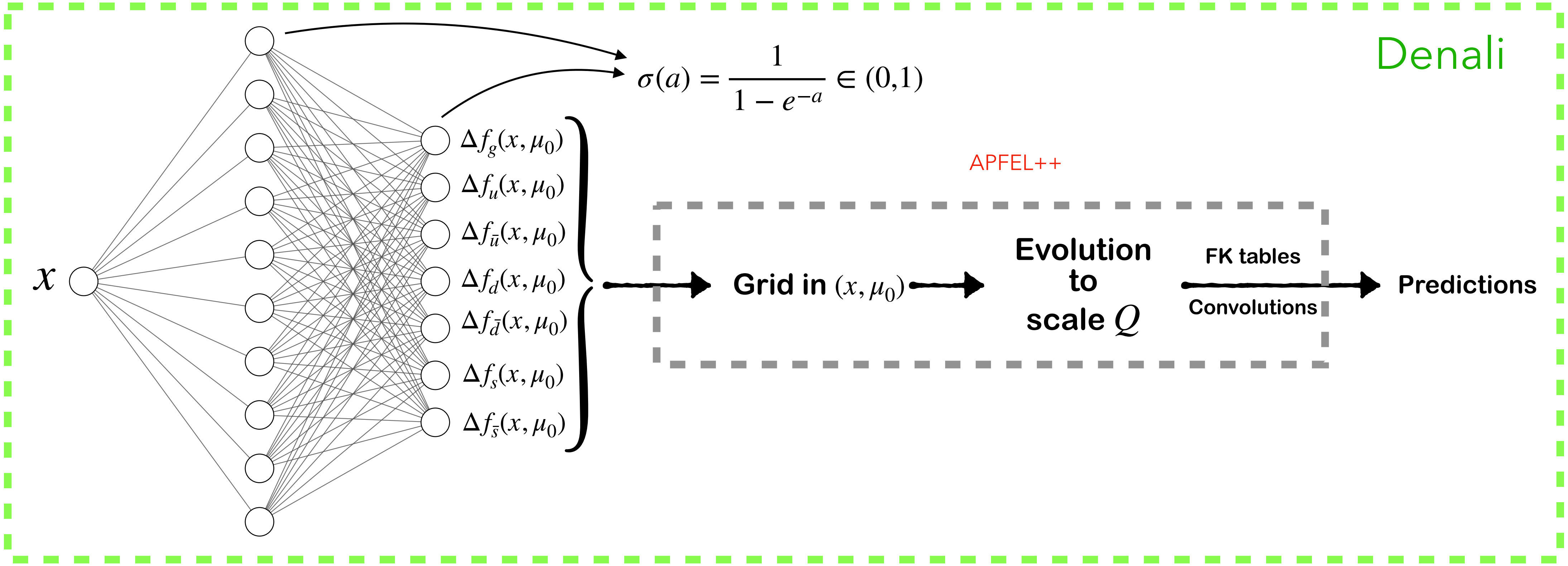

Theoretical constraints

Theoretical constraints

Positivity bound

Theoretical constraints

Positivity bound

More complicated beyond LO, but mild difference in the region where the bound is relevant (large-x)

Positivity of the cross sections implies LO bound for polarised PDFs

$$\left|\Delta f_i(x,Q^2)\right| \leq f_i(x,Q^2)\,, \quad \forall x\,, \forall Q^2\,,$$

[NPB 534 (1998) 227; arXiv:2401.10814]

Theoretical constraints

Positivity bound

More complicated beyond LO, but mild difference in the region where the bound is relevant (large-x)

Positivity of the cross sections implies LO bound for polarised PDFs

$$\left|\Delta f_i(x,Q^2)\right| \leq f_i(x,Q^2)\,, \quad \forall x\,, \forall Q^2\,,$$

[NPB 534 (1998) 227; arXiv:2401.10814]

Constraint enforced by construction by shifting and rescaling the output layers

$$\Delta f_i^{(k)}(x,Q_0^2) = \left[2\,\mathrm{NN}_i(x) - 1\right] f_i^{(U(1,100))}(x,Q_0^2)\,, \quad i = g, u, \bar{u}, d, \bar{d}, s, \bar{s}\,,$$

Theoretical constraints

Positivity bound

More complicated beyond LO, but mild difference in the region where the bound is relevant (large-x)

Positivity of the cross sections implies LO bound for polarised PDFs

$$\left|\Delta f_i(x,Q^2)\right| \leq f_i(x,Q^2)\,, \quad \forall x\,, \forall Q^2\,,$$

[NPB 534 (1998) 227; arXiv:2401.10814]

Constraint enforced by construction by shifting and rescaling the output layers

$$\Delta f_i^{(k)}(x,Q_0^2) = \left[2\,\mathrm{NN}_i(x) - 1\right] f_i^{(U(1,100))}(x,Q_0^2)\,, \quad i = g, u, \bar{u}, d, \bar{d}, s, \bar{s}\,,$$

Unpolarised PDF replica chosen at random for each polarised PDF replica

Theoretical constraints

Positivity bound

More complicated beyond LO, but mild difference in the region where the bound is relevant (large-x)

Positivity of the cross sections implies LO bound for polarised PDFs

$$\left|\Delta f_i(x, Q^2)\right| \leq f_i(x, Q^2)\,, \quad \forall x\,, \forall Q^2\,,$$

[NPB 534 (1998) 227; arXiv:2401.10814]

Constraint enforced by construction by shifting and rescaling the output layers

$$\Delta f_i^{(k)}(x, Q_0^2) = \left[2\,\mathrm{NN}_i(x) - 1\right] f_i^{(U(1,100))}(x, Q_0^2)\,, \quad i = g, u, \bar{u}, d, \bar{d}, s, \bar{s}\,,$$

Unpolarised PDF replica chosen at random for each polarised PDF replica

NNPDF31_(n)nlo_pch_as_0118 used as unpolarised set

Theoretical constraints

More complicated beyond LO, but mild difference in the region where the bound is relevant (large-x)

Positivity bound

Positivity of the cross sections implies LO bound for polarised PDFs

$$\left|\Delta f_i(x, Q^2)\right| \leq f_i(x, Q^2)\,, \quad \forall x\,, \forall Q^2\,,$$

[NPB 534 (1998) 227; arXiv:2401.10814]

Constraint enforced by construction by shifting and rescaling the output layers

$$\Delta f_i^{(k)}(x, Q_0^2) = \left[2\,\mathrm{NN}_i(x) - 1\right] f_i^{(U(1,100))}(x, Q_0^2)\,, \quad i = g, u, \bar{u}, d, \bar{d}, s, \bar{s}\,,$$

Unpolarised PDF replica chosen at random for each polarised PDF replica

NNPDF31_(n)nlo_pch_as_0118 used as unpolarised set

Sum rules

Theoretical constraints

More complicated beyond LO, but mild difference in the region where the bound is relevant (large-x)

Positivity bound

Positivity of the cross sections implies LO bound for polarised PDFs

$$\left|\Delta f_i(x,Q^2)\right| \leq f_i(x,Q^2)\,, \quad \forall x\,, \forall Q^2\,,$$

[NPB 534 (1998) 227; arXiv:2401.10814]

Constraint enforced by construction by shifting and rescaling the output layers

$$\Delta f_i^{(k)}(x,Q_0^2) = \left[2\,\mathrm{NN}_i(x) - 1\right] f_i^{(U(1,100))}(x,Q_0^2)\,, \quad i = g, u, \bar{u}, d, \bar{d}, s, \bar{s}\,,$$

Unpolarised PDF replica chosen at random for each polarised PDF replica

NNPDF31_(n)nlo_pch_as_0118 used as unpolarised set

Sum rules

Assumption of SU(2) and SU(3) as flavour symmetries

Theoretical constraints

More complicated beyond LO, but mild difference in the region where the bound is relevant (large-x)

Positivity bound

Positivity of the cross sections implies LO bound for polarised PDFs

$$\left|\Delta f_i(x,Q^2)\right| \leq f_i(x,Q^2)\,,\quad \forall x\,,\forall Q^2\,,$$

[NPB 534 (1998) 227; arXiv:2401.10814]

Constraint enforced by construction by shifting and rescaling the output layers

$$\Delta f_i^{(k)}(x,Q_0^2) = \left[2\,\mathrm{NN}_i(x) - 1\right] f_i^{(U(1,100))}(x,Q_0^2)\,,\quad i = g,u,\bar{u},d,\bar{d},s,\bar{s}\,,$$

Unpolarised PDF replica chosen at random for each polarised PDF replica

NNPDF31_(n)nlo_pch_as_0118 used as unpolarised set

Sum rules

Assumption of SU(2) and SU(3) as flavour symmetries

a_3 and a_8 from semi-leptonic β-decay introduced at data level

Scale-independent in $\overline{\mathrm{MS}}$, but computed at $Q^2 = 1\,\mathrm{GeV}^2$

$$a_3 = \int_0^1 dx\,\left[\Delta f_u^+(x,Q^2) - \Delta f_d^+(x,Q^2)\right] = 1.2756 \pm 0.0013$$

$$a_8 = \int_0^1 dx\,\left[\Delta f_u^+(x,Q^2) + \Delta f_d^+(x,Q^2) - 2\Delta f_s^+(x,Q^2)\right] = 0.585 \pm 0.025$$

[PTEP 2022 (2022) 083C01]

3. Results

Baseline: NNLO global set – a_3, a_8 and positivity imposed

Impact of NNLO corrections

Impact of NNLO corrections

Experiment	N_{dat}	baseline χ^2/N_{dat} NLO	baseline χ^2/N_{dat} NNLO
EMC	10	0.57	0.49
SMC	12	0.29	0.32
	12	1.34	1.20
E142	7	0.58	0.85
E143	25	0.74	0.69
	25	1.30	1.23
E154	11	0.22	0.20
E155	22	0.66	0.85
	22	0.71	0.81
COMPASS	17	0.58	0.95
	15	0.36	1.02
HERMES	8	0.22	0.27
	14	0.46	0.53
	14	0.63	0.74
JLAB-E06	1	0.72	0.86
JLAB-EG1	2	0.01	0.01
	1	0.01	0.01
COMPASS	12	2.32	2.01
	12	1.34	1.13
	12	0.69	0.94
	12	0.73	0.98
	12	0.31	1.23
	12	0.47	1.51
	12	0.40	0.40
	12	0.92	0.82
HERMES	9	1.90	2.05
	9	1.03	0.68
	9	0.35	1.53
	9	1.30	2.41
	9	1.48	1.72
	9	0.63	1.04
Total	362	0.64	0.78

Impact of NNLO corrections

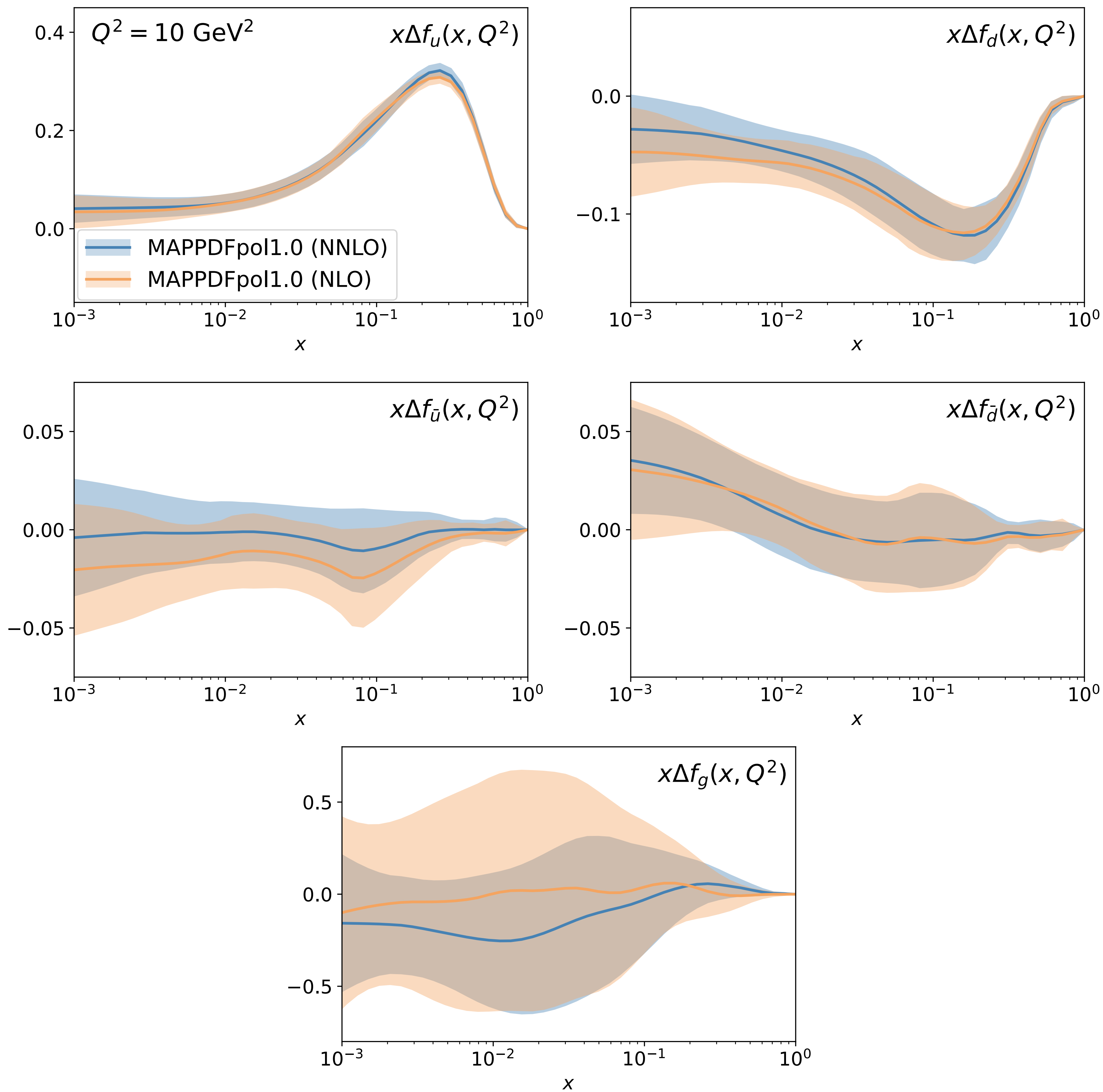

		baseline $\chi^2/N_{\rm dat}$	
Experiment	$N_{\rm dat}$	NLO	NNLO
EMC	10	0.57	0.49
SMC	12	0.29	0.32
	12	1.34	1.20
E142	7	0.58	0.85
E143	25	0.74	0.69
	25	1.30	1.23
E154	11	0.22	0.20
E155	22	0.66	0.85
	22	0.71	0.81
COMPASS	17	0.58	0.95
	15	0.36	1.02
HERMES	8	0.22	0.27
	14	0.46	0.53
	14	0.63	0.74
JLAB-E06	1	0.72	0.86
JLAB-EG1	2	0.01	0.01
	1	0.01	0.01
COMPASS	12	2.32	2.01
	12	1.34	1.13
	12	0.69	0.94
	12	0.73	0.98
	12	0.31	1.23
	12	0.47	1.51
	12	0.40	0.40
	12	0.92	0.82
HERMES	9	1.90	2.05
	9	1.03	0.68
	9	0.35	1.53
	9	1.30	2.41
	9	1.48	1.72
	9	0.63	1.04
Total	362	0.64	0.78

Impact of NNLO corrections - strangeness

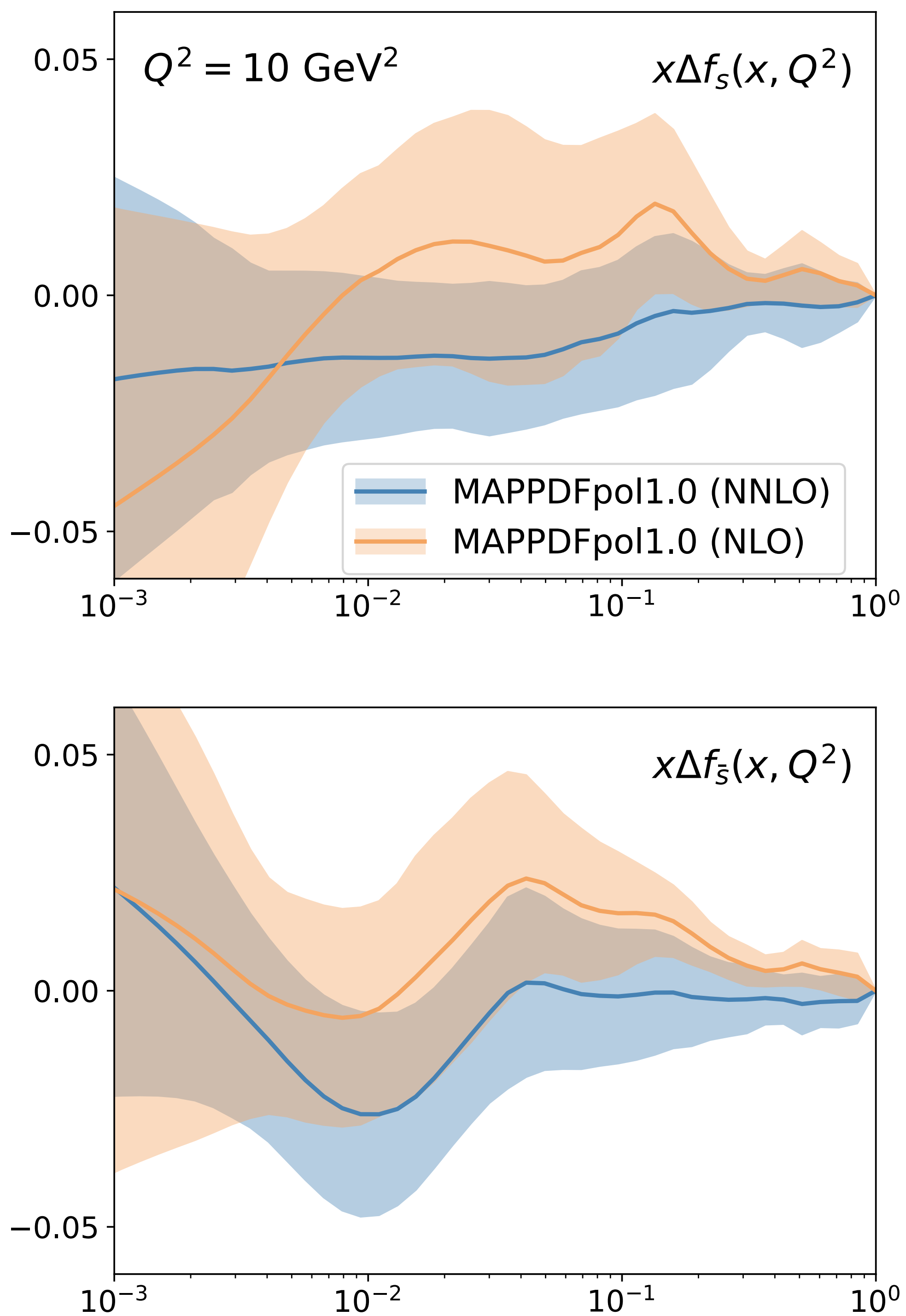

Experiment	$N_{\rm dat}$	baseline $\chi^2/N_{\rm dat}$ NLO	baseline $\chi^2/N_{\rm dat}$ NNLO
EMC	10	0.57	0.49
SMC	12	0.29	0.32
	12	1.34	1.20
E142	7	0.58	0.85
E143	25	0.74	0.69
	25	1.30	1.23
E154	11	0.22	0.20
E155	22	0.66	0.85
	22	0.71	0.81
COMPASS	17	0.58	0.95
	15	0.36	1.02
HERMES	8	0.22	0.27
	14	0.46	0.53
	14	0.63	0.74
JLAB-E06	1	0.72	0.86
JLAB-EG1	2	0.01	0.01
	1	0.01	0.01
COMPASS	12	2.32	2.01
	12	1.34	1.13
	12	0.69	0.94
	12	0.73	0.98
	12	0.31	1.23
	12	0.47	1.51
	12	0.40	0.40
	12	0.92	0.82
HERMES	9	1.90	2.05
	9	1.03	0.68
	9	0.35	1.53
	9	1.30	2.41
	9	1.48	1.72
	9	0.63	1.04
Total	362	0.64	0.78

Impact of data

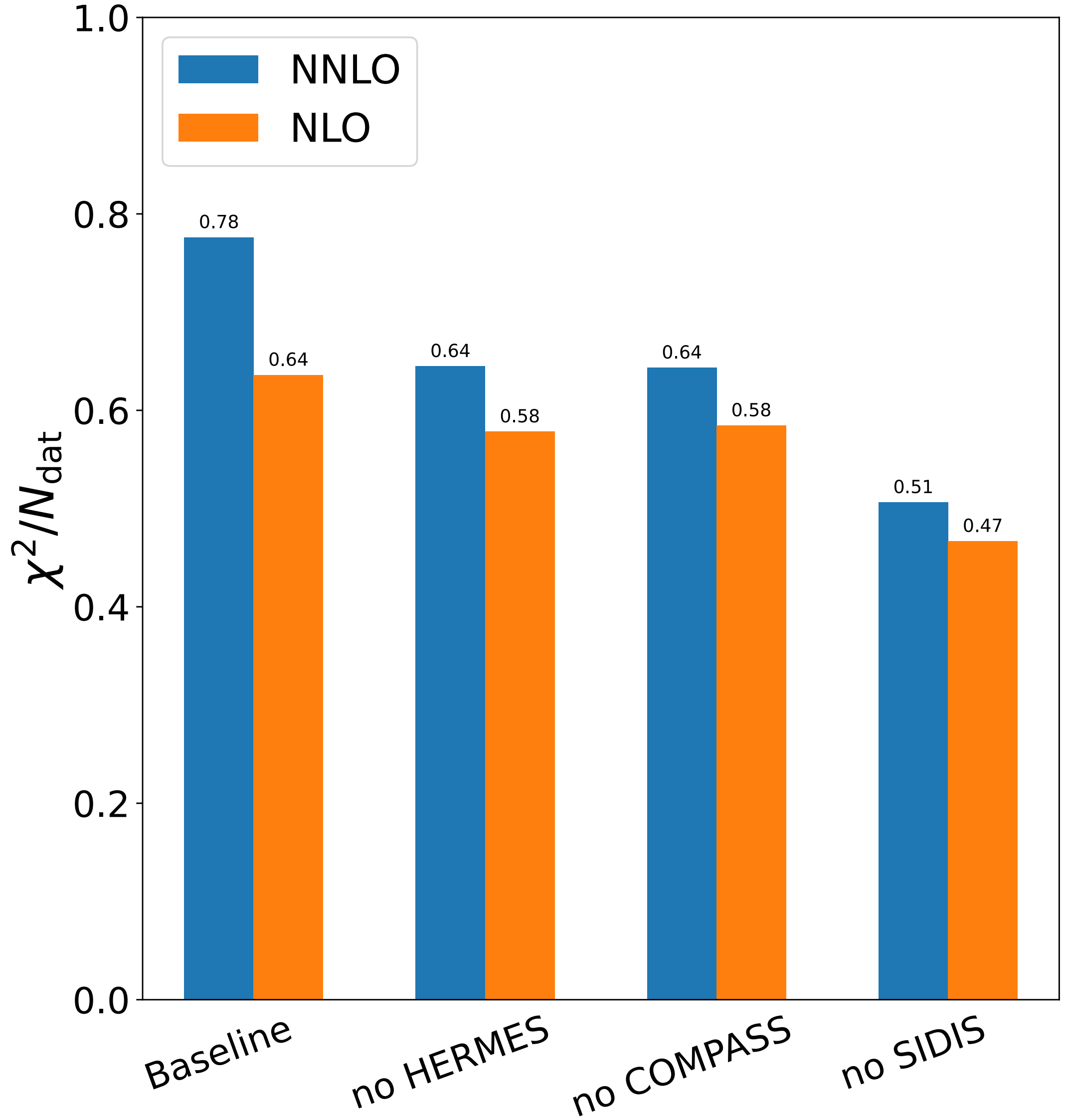

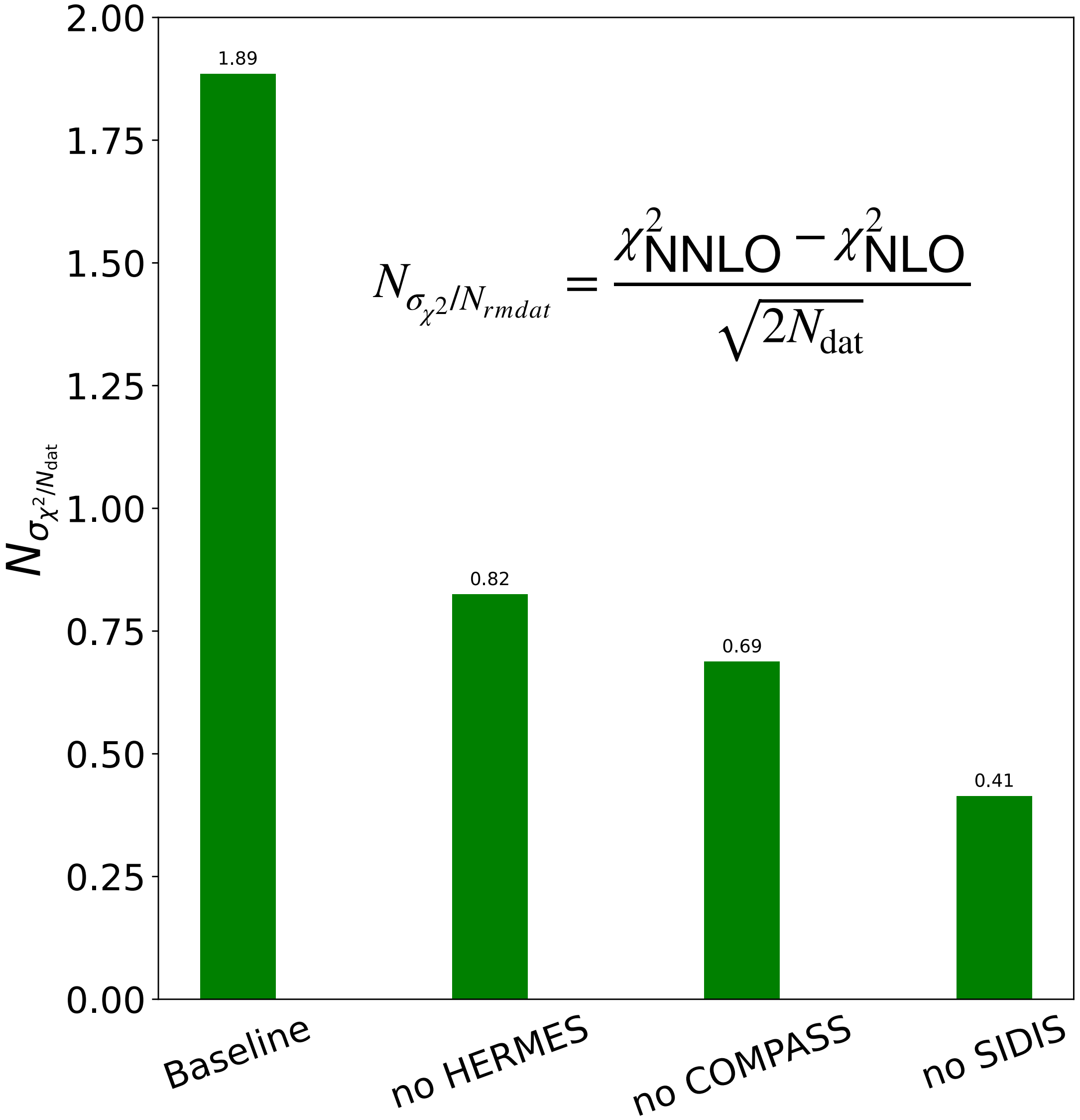

Worsening of the χ^2 at NNLO:

SIDIS data are not described as well as DIS data

COMPASS and HERMES SIDIS data may be in tension with each other

Sum rules

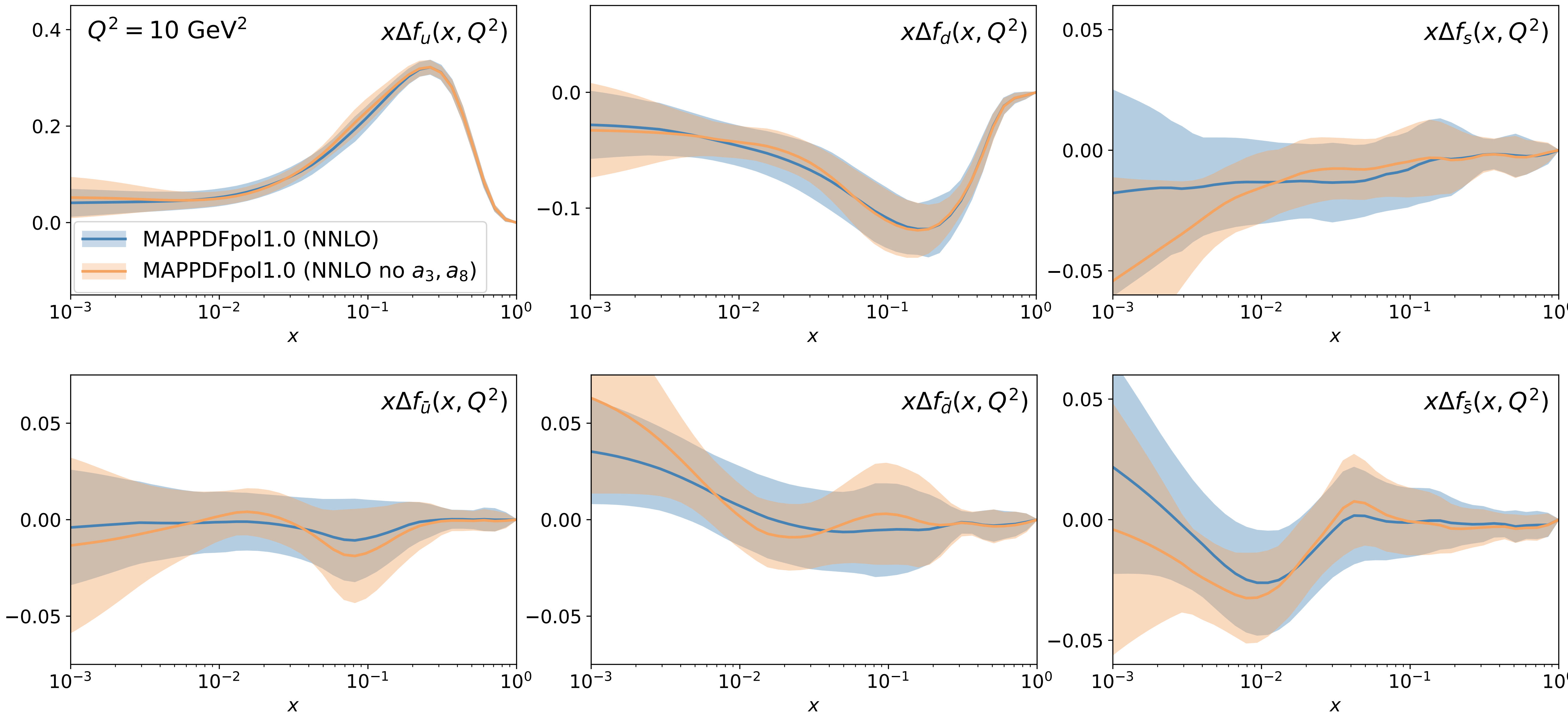

Baseline

$\chi^2/N_{\text{dat}} = 0.78$

No a_3 and a_8

$\chi^2/N_{\text{dat}} = 0.74$

Sum rules

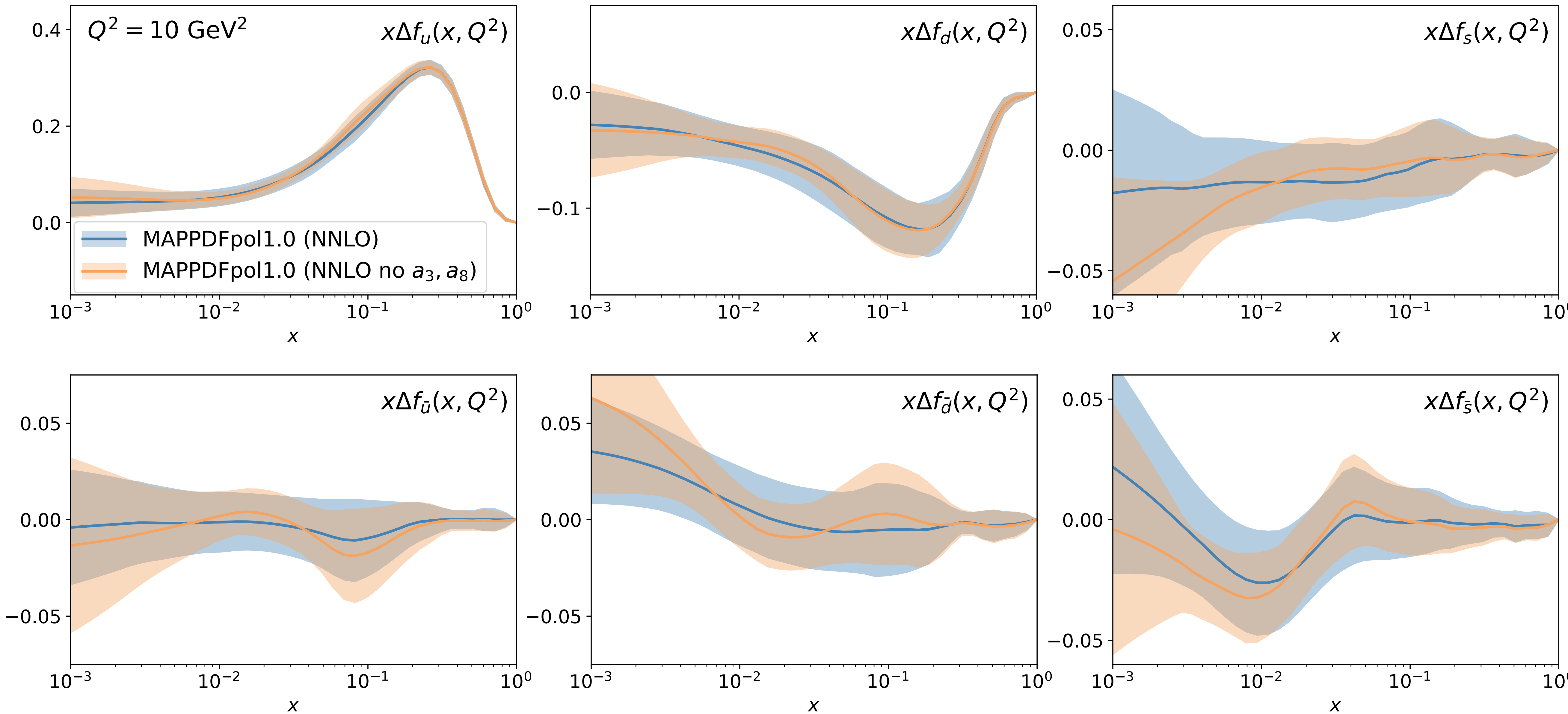

Baseline

$\chi^2/N_{\rm dat} = 0.78$

No a_3 and a_8

$\chi^2/N_{\rm dat} = 0.74$

the impact of sum rules is moderate

Data sets compatible with SU(2) and SU(3) flavour symmetries

Positivity bound

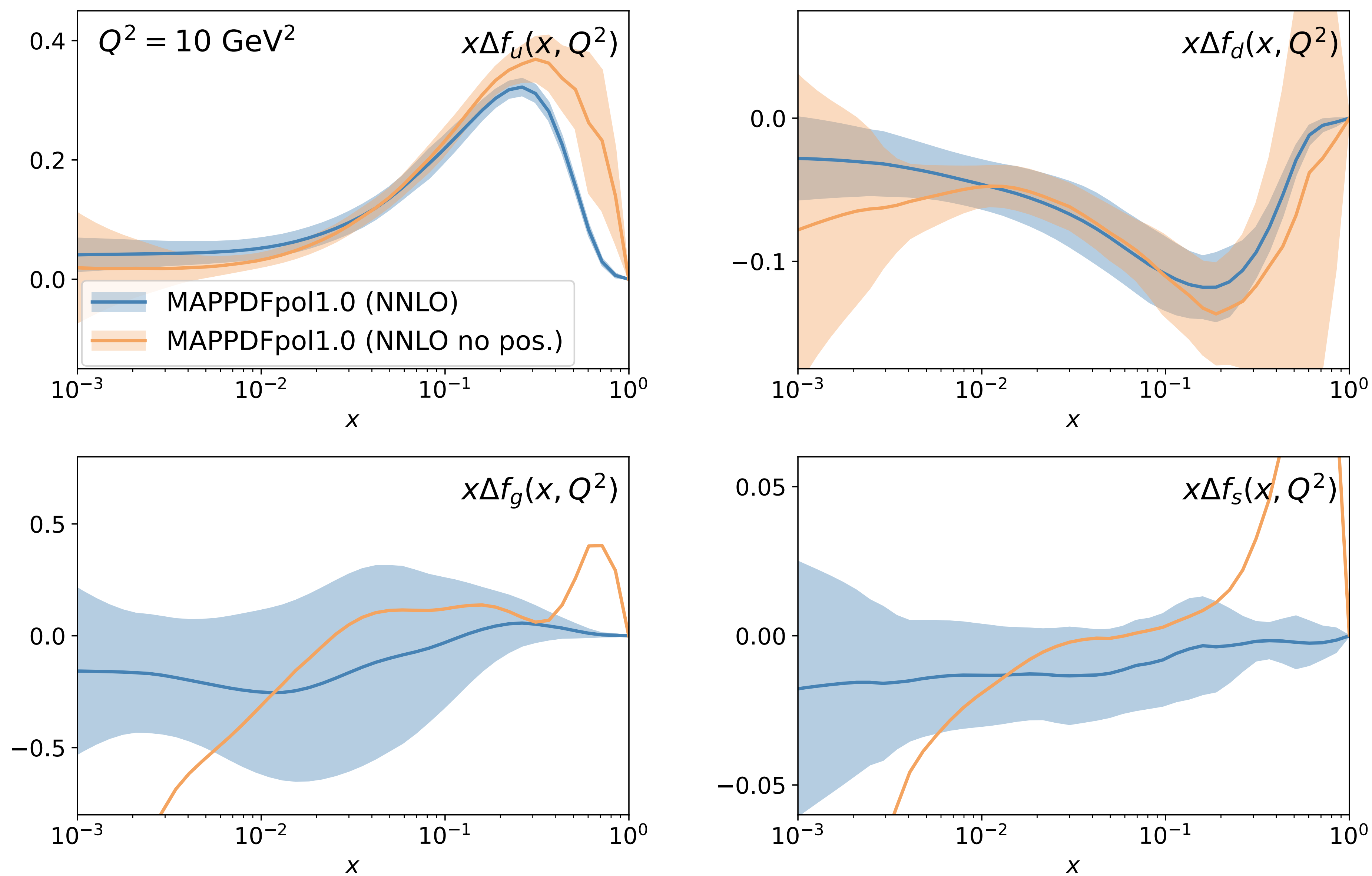

$$\Delta f_i^{(k)}(x, Q_0^2) = \left[2\,\mathrm{NN}_i(x) - 1\right]\left[f_i^{(0)}(x, Q_0^2) + 50\,\sigma_i(x, Q_0^2)\right]$$

Baseline	**No positivity**
$\chi^2/N_{\rm dat} = 0.78$	$\chi^2/N_{\rm dat} = 0.66$

Positivity bound

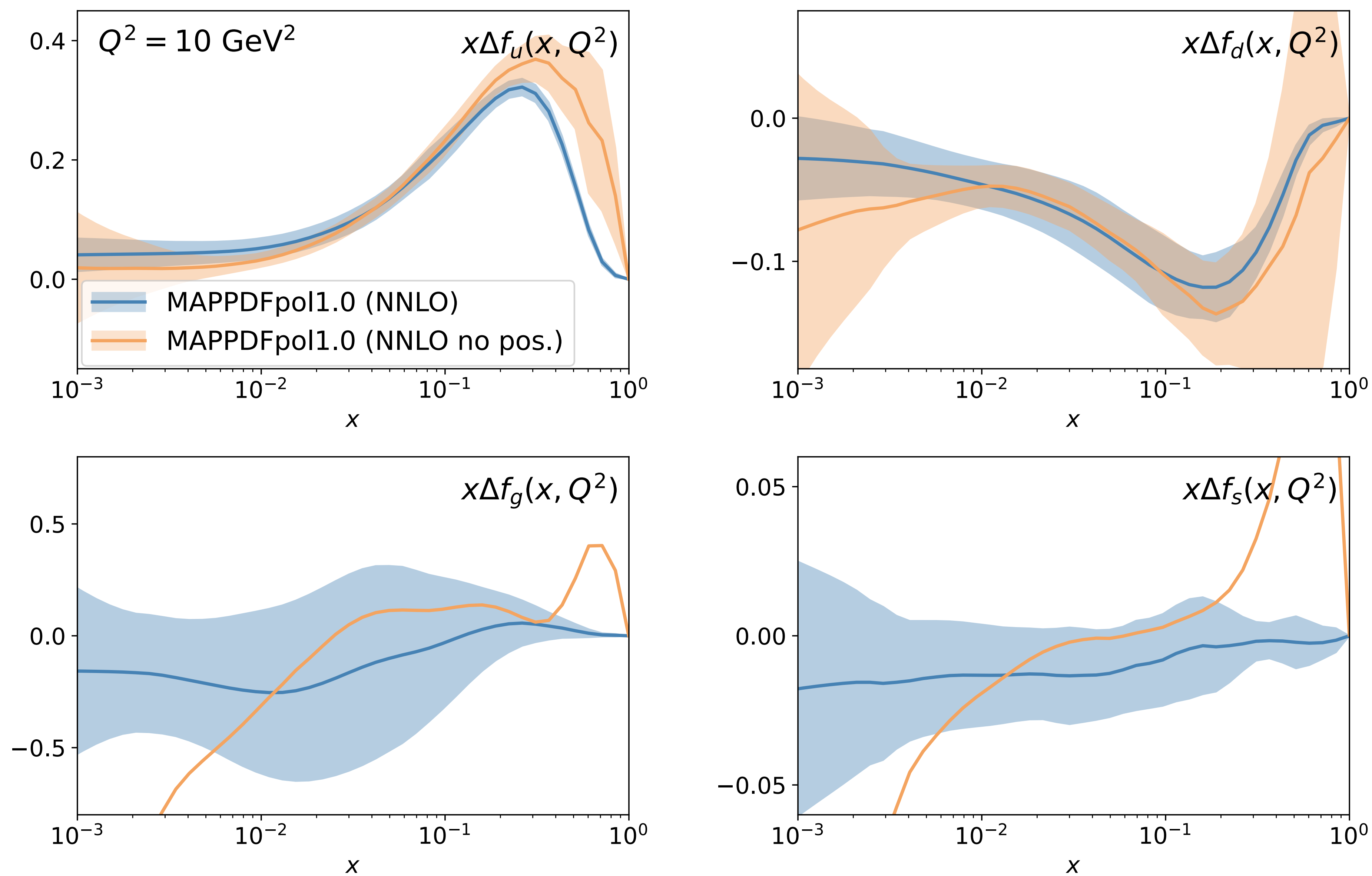

$$\Delta f_i^{(k)}(x, Q_0^2) = \left[2\,\mathrm{NN}_i(x) - 1\right]\left[f_i^{(0)}(x, Q_0^2) + 50\,\sigma_i(x, Q_0^2)\right]$$

Baseline	**No positivity**
$\chi^2/N_{\rm dat} = 0.78$	$\chi^2/N_{\rm dat} = 0.66$

Positivity relevant at large-x, where data is lacking

4. Conclusions

Summary and outlook

Results

NNLO corrections are generally moderate

Sea quark and gluon PDFs remain unconstrained and compatible with zero

Strangeness compatible with zero in DIS and SIDIS, no signs of strange asymmetry

Non-trivial interplay between NNLO corrections and SIDIS experimental data

No sign of SU(2) and SU(3) violation from the data

Future improvements

Extend to gauge boson production in polarised p-p collisions (sea quarks)

Double-spin asymmetry in inclusive hadron and jets production (gluon)

Theory uncertainties – MHOUs and nuclear corrections

Summary and outlook

Results

NNLO corrections are generally moderate

Sea quark and gluon PDFs remain unconstrained and compatible with zero

Strangeness compatible with zero in DIS and SIDIS, no signs of strange asymmetry

Non-trivial interplay between NNLO corrections and SIDIS experimental data

No sign of SU(2) and SU(3) violation from the data

Future improvements

Extend to gauge boson production in polarised p-p collisions (sea quarks)

Double-spin asymmetry in inclusive hadron and jets production (gluon)

Theory uncertainties – MHOUs and nuclear corrections

Thank you

Backup slides

Tension between DIS and SIDIS?

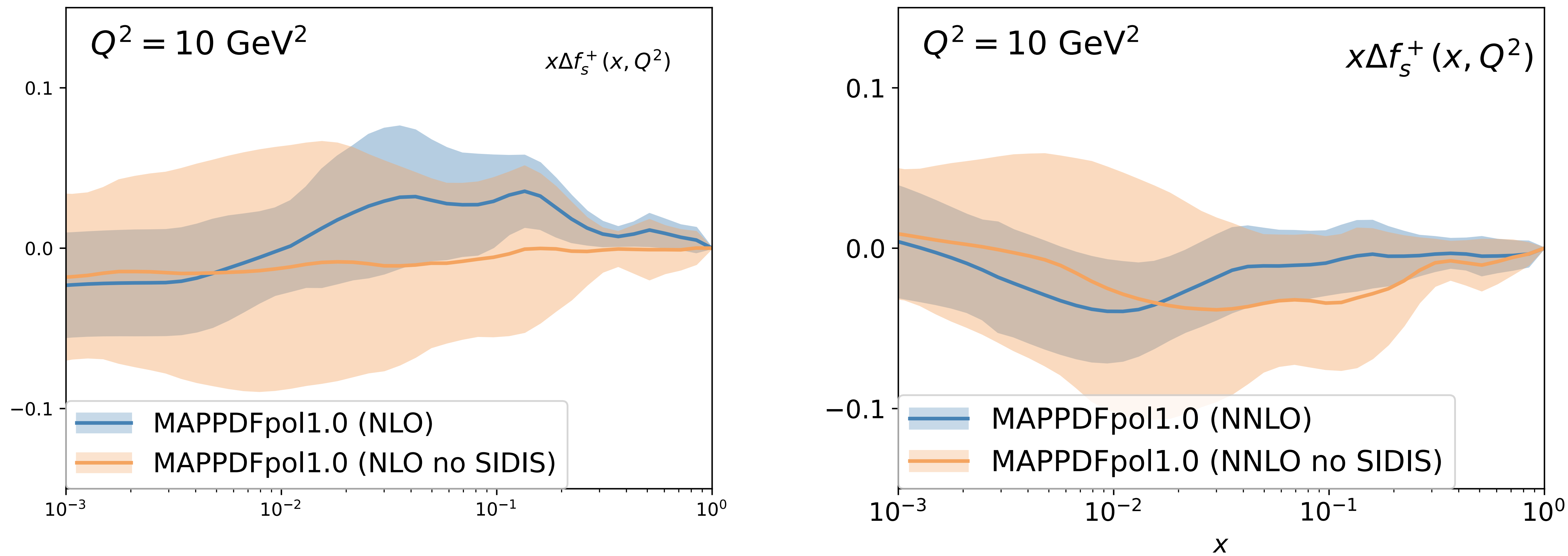

Reduction of uncertainties for strangeness when SIDIS included (NLO and NNLO)

Determination with SIDIS data still compatible with the global one

Strangeness compatible with zero within (large) uncertainties

Follow-up: SIDIS and NNLO

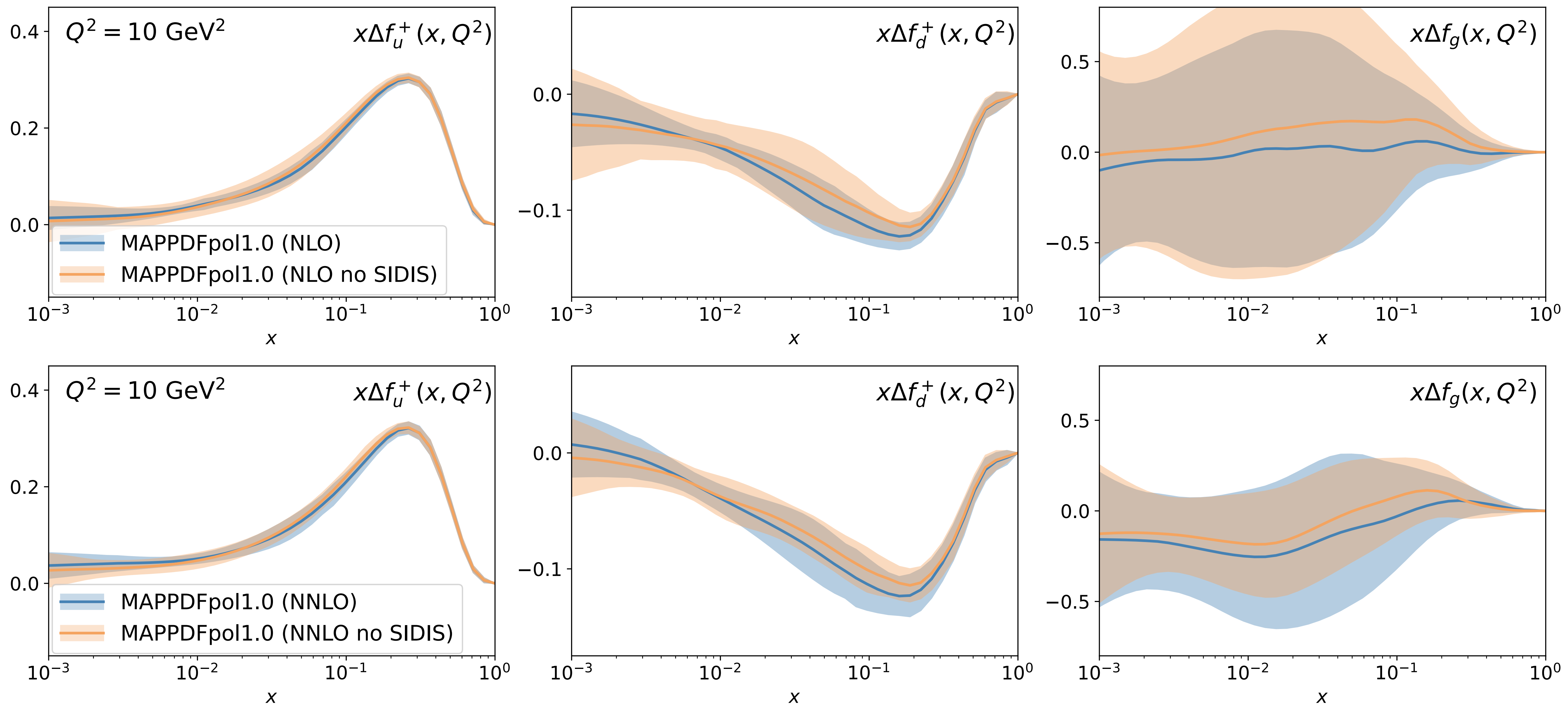

SIDIS has different impact at NLO and NNLO

uncertainties for u^+, d^+ reduces at NLO, but increase at NNLO

The gluon is left unaltered

Polarised charm at NNLO

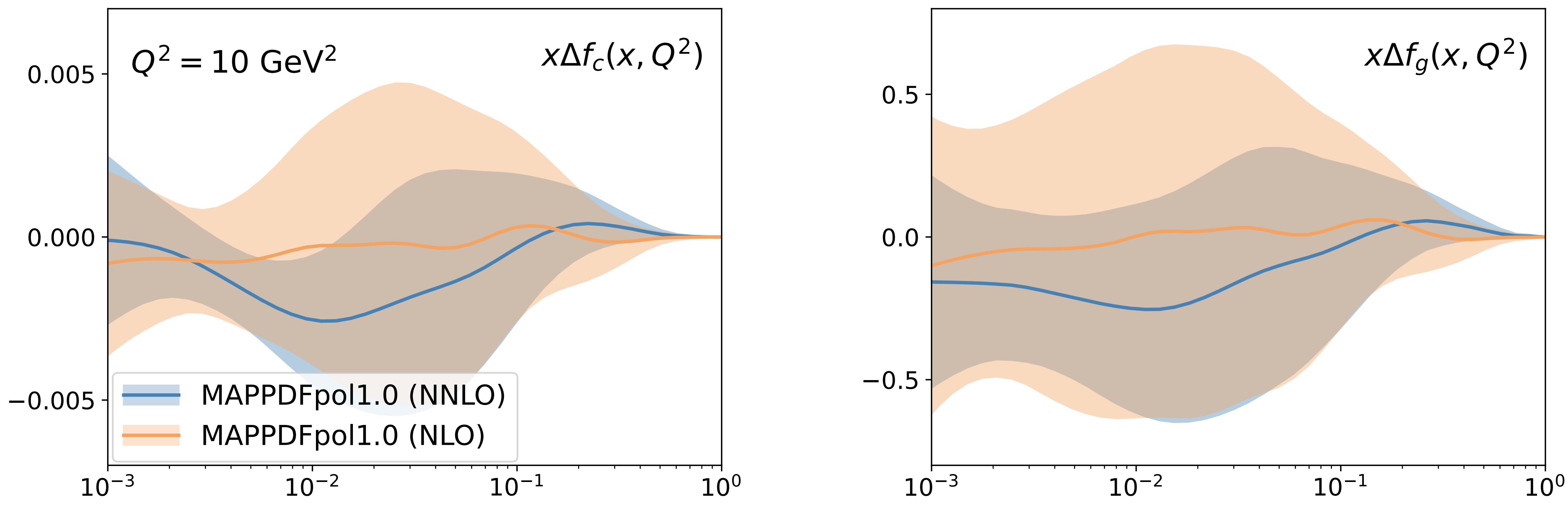

DIS data

Experiment	Set	$N_{\rm dat}$	$x_{\rm min}$	$x_{\rm max}$	$Q^2_{\rm min}$[GeV^2]	$Q^2_{\rm max}$[GeV^2]	F	Ref.
E142								
	E142-G1N	8 (7)	.035	.466	1.1	5.5	g_1	PRL 71 (1993) 659
E143								
	E143-G1D	28 (25)	.031	.749	1.27	9.52	g_1	PRD 58 112003
	E142-G1P	28 (25)	.035	.466	1.27	9.52	g_1	PRD 58 112003
E154								
	E154-G1N	11	.017	.024	1.2	15.0	g_1	PRL 79 (1997) 26
E155								
	E155-A1P	24 (22)	.015	.750	1.22	34.72	g_1/F_1	PLB 493 (2000) 19
	E155-A1N	24 (22)	.015	.750	1.22	34.72	g_1/F_1	PLB 493 (2000) 19
EMC								
	EMC-G1P	10	.015	0.466	3.5	29.5	g_1	NPB 328 (1989) 1
JLAB E06 014								
	JLAB-A1N	6 (1)	.277	0.548	3.078	3.078	g_1/F_1	PRD 94 052003
JLAB E97 103								
	JLAB-E97-103-G1N	5 (0)	.160	.200	0.57	1.34	g_1	AIP CP 675 1 615
JLAB E99 117								
	JLAB-E99-117-G1N-F1N	3 (0)	.33	.60	2.71	4.83	g_1/F_1	PRC 70 065207
JLAB EG1 DVCS-D								
	JLAB-EG1-DVCS-G1D-F1D	44 (1)	.158	0.574	1.078	4.666	g_1/F_1	PRC 90 025212
	JLAB-EG1-DVCS-G1P-F1P	47 (2)	.154	0.578	1.064	4.115	g_1/F_1	PRC 90 025212
SMC								
	SMC-G1D	13 (12)	.002	.48	0.50	54.80	g_1	PRD 60 079902
	SMC-G1P	13 (12)	.002	.48	0.50	54.80	g_1	PRD 60 079902
COMPASS-D								
	CMP07-G1D	15	.0046	0.567	1.1	60.8	g_1	PRL 647 (2007) 8
COMPASS-P								
	CMP10-G1P	17	.0036	.57	1.1	67.4	g_1	PRL 690 (2010) 466
HERMES97								
	HERMES-G1N	9 (8)	.033	.464	1.22	5.25	g_1	PLB 404 (1997) 383
HERMES								
	HERMES-G1P	15 (14)	.0264	.7248	1.12	12.21	g_1	PRD 75 012007
	HERMES-G1D	15 (14)	.0264	.7248	1.12	12.21	g_1	PRD 75 012007
Total DIS		335 (218)						

SIDIS data

Experiment	Set	N_{dat}	x_{min}	x_{max}	Q^2_{min} [GeV^2]	Q^2_{max} [GeV^2]	F	Ref.
COMPASS-P								
	COMPASS-A1P-KA-MINUS	12	.004	.7	1.16	55.6	$g_1^{(h)}/F_1^{(h)}$	PLB 693 (2010) 227
	COMPASS-A1P-KA-PLUS	12	.004	.7	1.16	55.6	$g_1^{(h)}/F_1^{(h)}$	PLB 693 (2010) 227
	COMPASS-A1P-PI-MINUS	12	.004	.7	1.16	55.6	$g_1^{(h)}/F_1^{(h)}$	PLB 693 (2010) 227
	COMPASS-A1P-PI-PLUS	12	.004	.7	1.16	55.6	$g_1^{(h)}/F_1^{(h)}$	PLB 693 (2010) 227
COMPASS-D								
	COMPASS-A1D-KA-MINUS	10	.004	.7	1.16	32.8	$g_1^{(h)}/F_1^{(h)}$	PLB 693 (2010) 227
	COMPASS-A1D-KA-PLUS	10	.004	.7	1.16	32.8	$g_1^{(h)}/F_1^{(h)}$	PLB 693 (2010) 227
	COMPASS-A1D-PI-MINUS	10	.004	.7	1.16	32.8	$g_1^{(h)}/F_1^{(h)}$	PLB 693 (2010) 227
	COMPASS-A1D-PI-PLUS	10	.004	.7	1.16	32.8	$g_1^{(h)}/F_1^{(h)}$	PLB 693 (2010) 227
HERMES-P								
	HERMES-2018-A1P-PI-MINUS	9	.033	.449	1.22	10.28	$g_1^{(h)}/F_1^{(h)}$	PRD 71 012003
	HERMES-2018-A1P-PI-PLUS	9	.033	.449	1.22	10.17	$g_1^{(h)}/F_1^{(h)}$	PRD 71 012003
HERMES-D								
	HERMES-2018-A1D-KA-MINUS	9	.033	.449	1.21	10.01	$g_1^{(h)}/F_1^{(h)}$	PRD 71 012003
	HERMES-2018-A1D-KA-PLUS	9	.033	.449	1.21	10.07	$g_1^{(h)}/F_1^{(h)}$	PRD 71 012003
	HERMES-2018-A1D-PI-MINUS	9	.033	.449	1.21	9.97	$g_1^{(h)}/F_1^{(h)}$	PRD 71 012003
	HERMES-2018-A1D-PI-PLUS	9	.033	.449	1.21	9.92	$g_1^{(h)}/F_1^{(h)}$	PRD 71 012003
Total SIDIS		142						
Total DIS + SIDIS		477 (360)						

Choosing the number of replicas

N_{rep} determined requiring statistical features of the data reproduced by the ensemble with relative accuracy below 1%

$$\left\langle F_i^{(art)} \right\rangle_{rep} = \frac{1}{N_{rep}} \sum_{k=1}^{N_{rep}} F_i^{(art)(k)} \qquad \sigma_i^{(art)} = \sqrt{\left\langle \left(F_i^{(art)} \right)^2 \right\rangle_{rep} - \left\langle F_i^{(rep)} \right\rangle_{rep}^2}$$

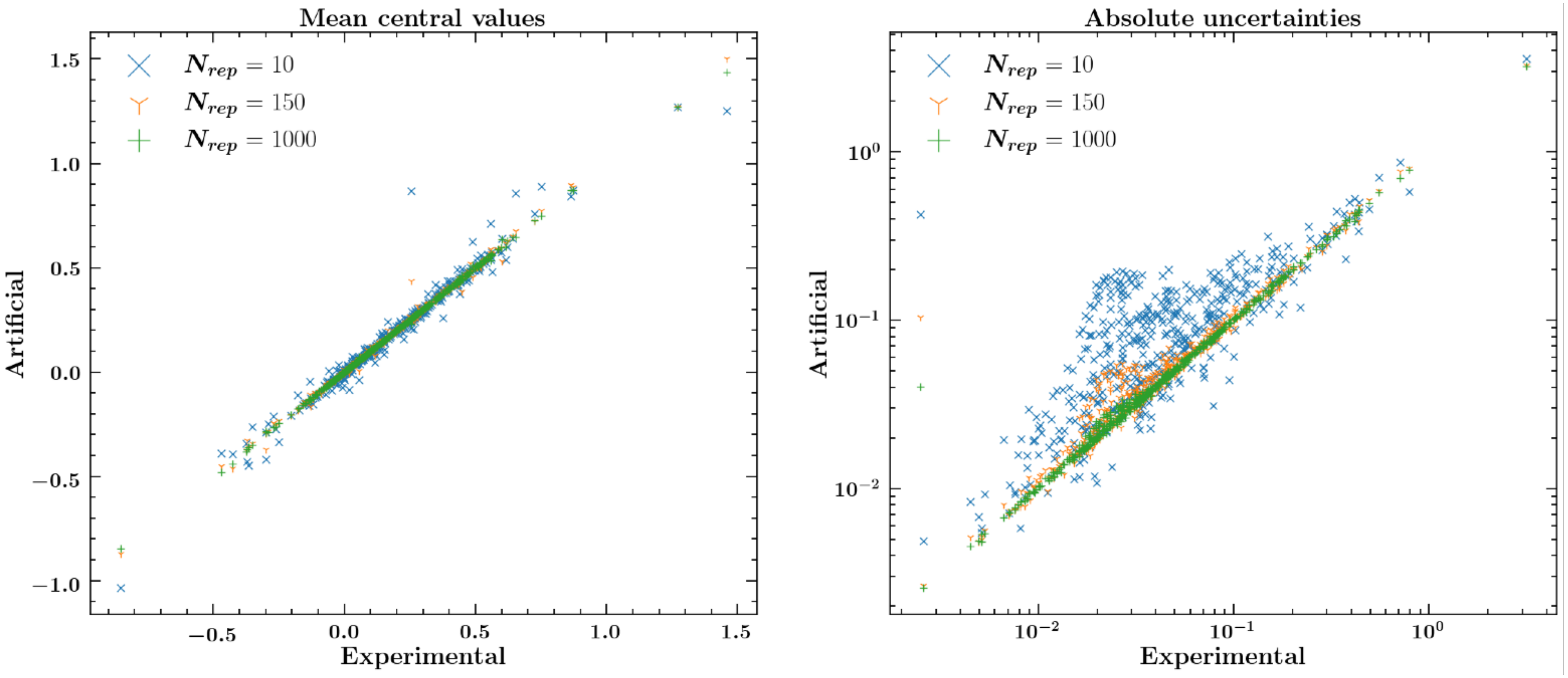

Optimisation

Levenberg-Marquardt algorithm (Ceres Solver) to minimise the error function

$$E^{(k)}_{\mathrm{tr,val}} = \frac{1}{N_{\mathrm{tr,val}}} \sum_{i,j=1}^{N_{\mathrm{tr,val}}} \left(g_i^{(net)(k)} - g_i^{(art)(k)} \right) \left(\mathrm{cov}^{-1}\right)_{ij} \left(g_j^{(net)(k)} - g_j^{(art)(k)} \right)$$

Cross-validation splits dataset in training (80%) and validation (20%)

Error function computed for both, but minimised on the training set

Best-fit corresponds to the minimum of the error function in the validation set

Optimisation

Levenberg-Marquardt algorithm (Ceres Solver) to minimise the error function

$$E^{(k)}_{\mathrm{tr,val}} = \frac{1}{N_{\mathrm{tr,val}}} \sum_{i,j=1}^{N_{\mathrm{tr,val}}} \left(g_i^{(net)(k)} - g_i^{(art)(k)} \right) \left(\mathrm{cov}^{-1} \right)_{ij} \left(g_j^{(net)(k)} - g_j^{(art)(k)} \right)$$

Cross-validation splits dataset in training (80%) and validation (20%)

Error function computed for both, but minimised on the training set

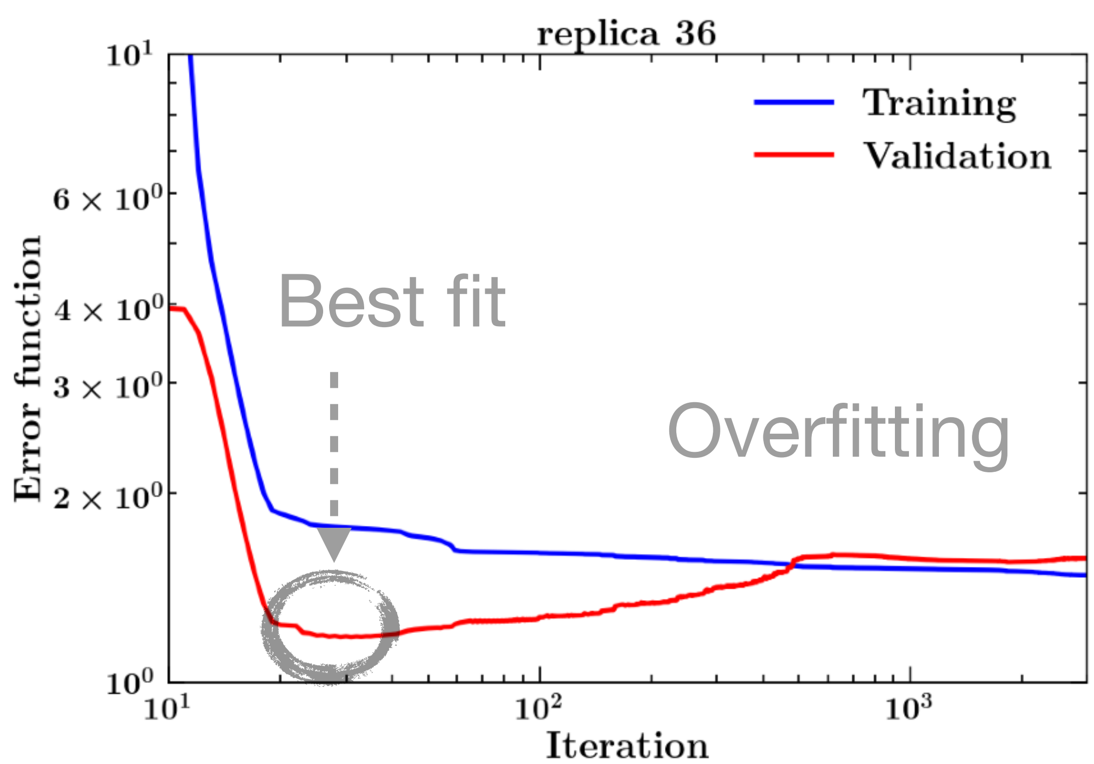

Best-fit corresponds to the minimum of the error function in the validation set